REPORT

FCR-N DESIGN OF REQUIREMENTS

VERSION 1 - 4 JULY 2017

AUTHORS

ROBERT ERIKSSON — SVENSKA KRAFTNÄT

NIKLAS MODIG — SVENSKA KRAFTNÄT

ANDREAS WESTBERG — SVENSKA KRAFTNÄT

Contents

ENTSO-E AISBL • Avenue Cortenbergh 100 • 1000 Brussels • Belgium • Tel +32 2 741 09 50 • Fax +32 2 741 09 51 • info@entsoe.eu • www.entsoe.eu

ABBREVIATIONS AND SYMBOLS

TABLE 1. ABBREVIATIONS AND SYMBOLS

aFRR		Automatic frequency restoration reserve
FCP		Frequency containment process
FCR-D		Frequency Containment Reserve for Disturbances
FCR-N		Frequency Containment reserve for normal operation
FFT		Fast Fourier transform
KPI		Key performance indicator
PSD		Power spectral density
pu		Per unit
SISO		Single-input-single-output
α		Backlash scaling factor
*A*m [°]		Amplitude margin (also gain margin)
b [%]		Backlash (defined as ± e.i. the total is 2b)
D(s)		Transfer function of disturbance (from white noise)
d [MW]		Power disturbance
E_{k-low} [MWs]		Kinetic inertia of the low inertia system
E_{k-avg} [MWs]		Kinetic inertia of the average inertia system
e		White noise
e_p [%]		Droop
Δf [Hz]		Grid frequency deviation
df [Hz]		Limit of the grid frequency deviation
$F(s)$		Control unit – Transfer function of the FCR response
f_0 [Hz]		Nominal grid frequency
φ_{m}		Phase margin
$G_0(s)$		Loop gain
$G_{\mathrm{min}}(s)$ [Hz/MW]		Transfer function of the low inertia system
$G_{\mathrm{avg}}(s)$ [Hz/MW]		Transfer function of the average inertia system
H_{min} [s]	$H_{\mathrm{min}} = E_{k-\mathrm{min}}/S_{n-\mathrm{min}}$	Inertia constant of the low inertia system
H_{avg} [s]	$H_{\mathrm{avg}} = E_{k-\mathrm{avg}}/S_{n-\mathrm{avg}}$	Inertia constant of the average inertia system
H_x [s]		Inertia constant of machine *x*
k_{min} [%/Hz]		Load frequency dependency of the minimum system
k_{avg} [%/Hz]		Load frequency dependency of the average system
K_{p} [pu]		Proportional parameter in the PI controller
K_{i} [1/s]		Integrator part in the PI controller
M_{s}		Maximum sensitivity
$P_{\mathrm{e}x}$ *[MW]*		Electrical power of machine *x*
$P_{\mathrm{m}x}$ *[MW]*		Mechanical power of machine *x*
ΔP [MW]		Total volume FCR in steady state
r		Circle radius (stability margin)
$S_{\mathrm{n-min}}$ [MW]		System loading and power base of the low inertia system
$S_{\mathrm{n-avg}}$ [MW]		System loading and power base of the average inertia system
$s = j\omega$		Laplace operator and complex frequency, respectively
$S_{\mathrm{n-FCR}}$ [MVA]		Individual rating of a unit *n*
$S(s)$		Sensitivity function
T_{s} [s]		Gate servo time constant
T_{w} [s]		Water way time constant
w		White noise
$j\omega$		Complex angular frequency
$\emptyset_{\mathrm{w}}$		Power spectral density
θ_x		Angle of machine *x*

CONSTRAINTS

TABLE 2. SPECIFIED CONSTRAINTS

Parameter	Value
$E_{\mathrm{k-min}}$	120 GWs

$E_{\mathrm{k-avg}}$		190 GWs
df		0.1 Hz
f_0		50 Hz
φ_{m}		25°
G_o		No poles in the right half plane (RHP)
H_{min}	$H_{\mathrm{min}} = E_{\mathrm{k-min}}/S_{\mathrm{n-min}}$	5.2 s
H_{avg}	$H_{\mathrm{avg}} = E_{\mathrm{k-avg}}/S_{\mathrm{n-avg}}$	4.5 s
k_{min}		0.5 %/Hz
k_{avg}		1 %/Hz
M_{s}		2.31 dB
ΔP		600 MW
$S_{\mathrm{n-min}}$		23 GVA
$S_{\mathrm{n-avg}}$		42 GVA
T_{s}		0.2 s
T_{w}		1.5 s
$\emptyset_{\mathrm{w}}$		1

1. INTRODUCTION

Frequency quality is a measure of the power balancing in a synchronous system. The balancing is driven by variations in production and consumption, together with the control response of the reserves and inertia. The frequency quality in the Nordic system has reduced over the last years indicated by increased minutes outside normal band. The normal frequency band is 50±0.1 Hz which should not be exceeded more than 10 000 minutes per year. The frequency containment reserve for normal operation (FCR-N) is to handle the short term stochastic net power variation in production and consumption. Recently, secondary control, automatic frequency restoration reserve (aFRR) has been introduced in order to improve the quality but is not seen as the sole solution of the problem. Revision of the FCR-N in order move towards better quality is a complementary solution. One aim of the frequency containment process project (FCP project) is to develop thorough requirements on the FCR-N ancillary service to ensure good frequency quality. This document describes steps that have been taken to create the new FCR-N requirements.

1.1 BACKGROUND OF THE PROJECT

The FCP project stems from a project series named "*Measures to mitigate frequency oscillations with a time period of 40-90 s*" (commonly known as the *60 s-project*), which in turn consisted of phase 1 and phase 2. The 60 s-projects investigated how FCR-N was implemented practically within the Nordic region. The reason was that from a top-down viewpoint it was thought that the specification for FCR-N was fairly transparent and straight forward. From a bottoms-up viewpoint the specifications were though anything but consistent throughout the Nordic synchronous area resulting in various different implementations. It was thus decided that a new requirement shall also try to harmonize the practical implementation of FCR within the Nordic synchronous area.

The 60 s-project also included physical testing of hydro units that provided FCR. Twelve different hydro power stations were tested with various testing procedures such as frequency step response tests and sine-in-sine-out tests. For linear systems one can inject a sinusoidal signal and measure the output, which also is sinusoidal, but its amplitude and phase may have shifted. The

ENTSO-E AISBL • Avenue Cortenbergh 100 • 1000 Brussels • Belgium • Tel +32 2 741 09 50 • Fax +32 2 741 09 51 • info@entsoe.eu • www.entsoe.eu

sine-in-sine-out tests were performed in open loop by injection of an artificial frequency signal in the governor, i.e. a super imposed sinusoidal frequency signal fed into the governor. From this, transfer functions were estimated and stability in closed loop system was analysed. During these tests much new knowledge was gained in how the FCR requirements were implemented in practice, some were good and some were not. An example of the difference in implementation is shown in Figure 1 where in total 39 different sine-sweep tests using the twelve different hydro power stations are presented in a discrete Nyquist-like graph[i]. Each dashed curve is a test, at a hydro power plant, excited by a set of sinusoidal signals with different time periods injected into the governor. The response of the Nyquist curve at discrete frequencies is marked with 'x' and linear interpolation has been applied in between. Ideally, a curve should not enter the black circle and shall not appear on the left hand side of the point -1 (red dot) by encircle this point. Such response acts de-stabilising, clearly, units that act destabilising could be identified. Figure 2 shows two selected responses illustrating one response that stabilises the system (blue curve) and another that de-stabilises (red curve).

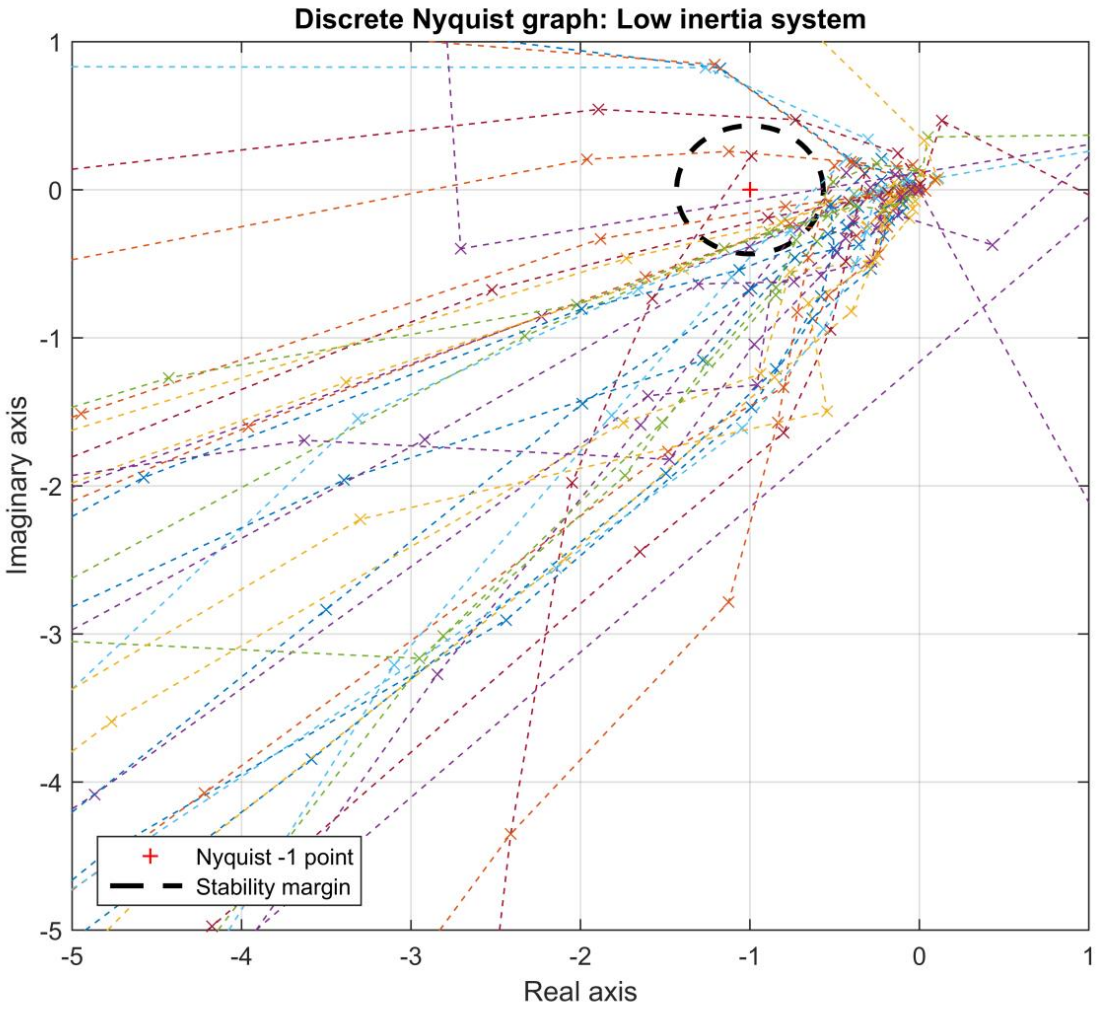

[i] The graph is created by assuming that all FCR-N providers have the same dynamic response as the tested unit.

FIGURE 1. RESULT FROM SINE-SWEEP TESTS PERFORMED DURING THE 60S PHASE 1 AND 2 PROJECTS

The results from previous projects show that there is a clear need to physically test and verify the dynamic performance. The existing requirements state that a unit shall have full activation after 150-180 seconds from a stepwise change in the frequency within the normal operating band of the FCR-N. In Sweden there is an additional requirement that 63 % of the steady state power response shall be activated after 60 seconds. The sine-sweep tests clearly showed that there is some unwanted dynamic performance that can be seen with sine-sweep tests but not with step response tests that have previously been used in the Nordic synchronous area.

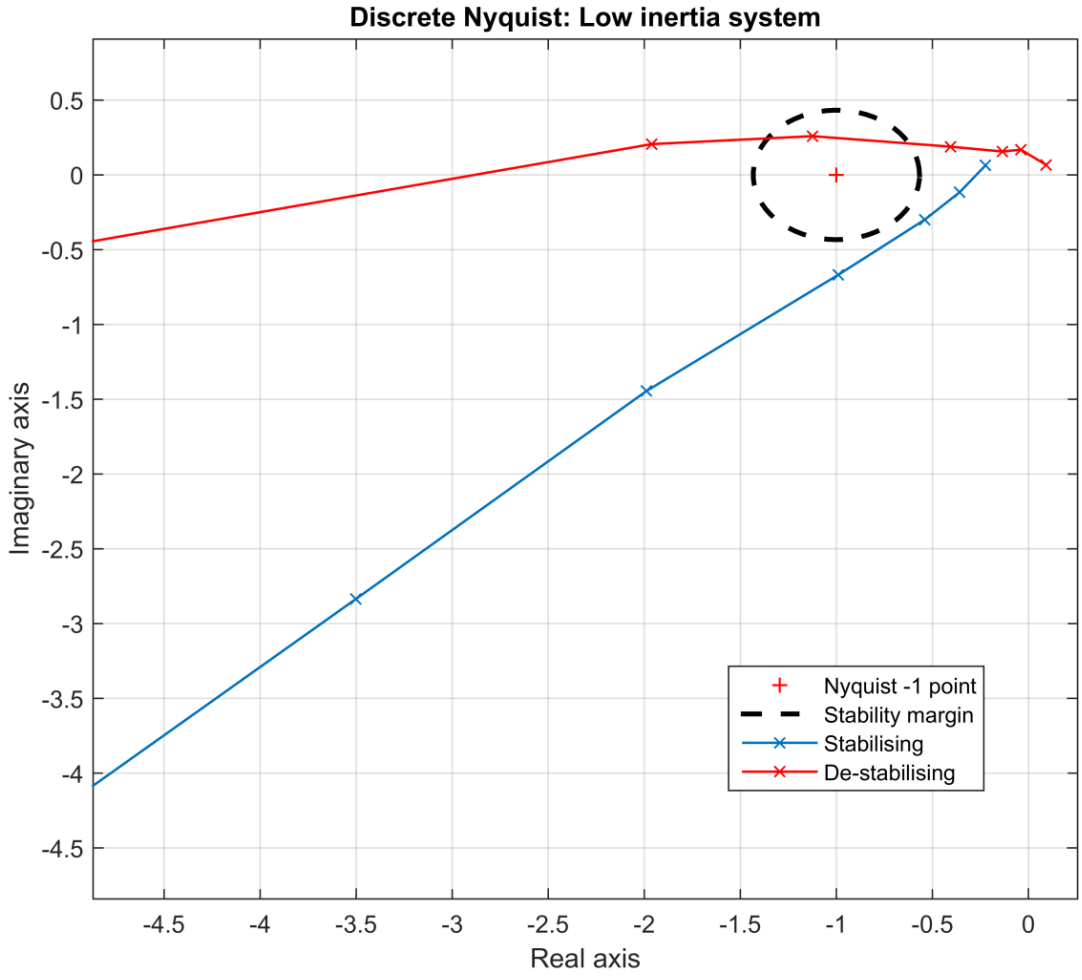

FIGURE 2. SELECTED RESPONSES FROM REAL TESTING, BLUE RESPONSE ACTS STABILISING AND RED ACTS DE-STABILISING.

1.2 SCOPE OF THE PROJECT – FCR-N

This work focuses on the design of the requirements of the FCR-N. The design shall consider the system need but is limited to technical limitations in hydro power units. Reasonable amount of hydro power units have to qualify in order to open up for enough capacity on the market and endorse competitive prices. The project aims not to revise the requirements on the aFRR but rather use the existing implementation to find proper shares between FCR-N and aFRR. The

project will only set the technical requirements for FCR-N and FCR-D products with constraints given. Impact from voltage dependency in loads, distributed inertia and activated network protections schemes are not considered. The analysis of the design is performed only on a linear single-input-single-output system with no voltage dependency but is verified in non-linear simulations.

1.3 GOALS

The goals are to come up with requirements on the FCR-N. The requirements shall

1. be functional and testable locally at each FCR provider,
2. specify dynamic response to ensure stability,
3. improve the frequency quality in relation to specified key performance indicators (KPIs) in relation to the system of today. The KPIs are to be specified in the project,
4. specify the dynamic response from net power variation to frequency deviation to meet the KPIs.

1.4 CONSTRAINTS

Constraints are given in Table 2.

1.5 OUTLINE

This document is organised as follows. In Section 2 a theoretical background is given for general control systems on the basis of transfer function with the concepts stability and performance. Next section provides the model description of an FCR-unit and different per unit scaling. The reference hydro power unit is also introduced which is used throughout the document. In Section 4 the requirements are described and motived, also results from simulations are provided. Section 5 gives an overview of real test procedure on site and how to achieve the response in order to verify qualification.

2. THEORETICAL BACKGROUND

In most physical systems non-linearities are to be considered in the control design. However, linear control design is often used and then verified by non-linear simulations and testing. This

ENTSO-E AISBL • Avenue Cortenbergh 100 • 1000 Brussels • Belgium • Tel +32 2 741 09 50 • Fax +32 2 741 09 51 • info@entsoe.eu • www.entsoe.eu

section describes linear control design for a single-input-single-output (SISO) system and how the non-linearity introduced by backlash can be included.

2.1 STABILITY

First some terminology on stability is used in terms of asymptotic stability which means that there exists no initial condition or no bounded input signal that drives the output to infinity.

Figure 3 shows a SISO system where *F(s)* is the transfer function of the control process, *G(s)* the plant, *d* is a disturbance signal entering the system, *y* is the output of the closed loop system *and s* is the Laplace operator.

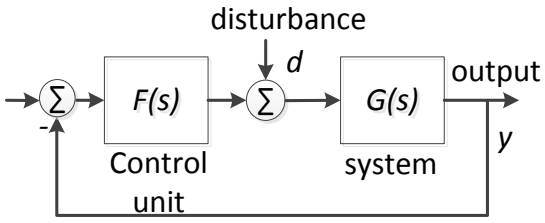

FIGURE 3. OVERVIEW OF A FEEDBACK SYSTEM

The aim is to determine whether or not the closed loop system is stable. The mathematical framework of transfer functions provides an elegant method, which is called *loop analysis*. The basic idea of loop analysis is to trace how a sinusoidal signal propagates in the feedback loop, this by investigating if the propagated signal grows or decays. One way to analyse stability is by using the Nyquist criterion which in turn uses the loop gain. The loop gain is defined as

$$G_O(s) = F(s)G(s). \tag{2.1}$$

The loop transfer function, also named sensitivity, is defined as

$$S(s) = \frac{1}{1+G_O(s)} \tag{2.2}$$

and describes the propagation of a signal through the loop i.e. how the output amplifies through the loop.

The amplification of a signal is determined by the denominator. Whether the signal grows as it is phase shifted by 180° (the signal has opposite sign) in the loop determines if the system is stable or not. The point where a signal has this phase shift and its amplitude remains (gain equals to one) corresponds to where to denominator is equal to zero i.e.

$$G_O(s)|_{s=j\omega_0} = -1. \tag{2.3}$$

At such conditions the signal grows to infinity, thus, the point -1 is of interest together with the loop gain.

The Nyquist curve is the loop gain, that can be plotted in the complex plane, with the Laplace operator *s* replaced by the complex value *jω* and ω varying as shown in Figure 4. The system is asymptotically stable if the Nyquist curve does not encircle the point -1. Basically, at the point where the Nyquist curve has a phase shift of 180° the loop transfer function should be smaller

than one. This holds true for simple enough systems (loop gains) as one could in reality cross the negative real axis twice to the left of the point -1 and still not encircle this point. Note that this is only valid if the loop gain is at least marginally stable i.e. no poles in the right half plane. For a more detailed description readers are referred to [1] and textbooks in the field of linear control theory. In practice it is not enough that a system is stable. There should also be some margins of stability that would describe how stable the system is and its robustness to perturbations. A stability margin is introduced by a distance between the Nyquist curve and the point -1. It can be specified in terms of amplitude margin[ii] (also known as gain margin), (A_m), phase margin[iii], (φ_m), and the smallest Euclidian distance, *r*, between the curve and the point -1 (referred to as the stability margin).

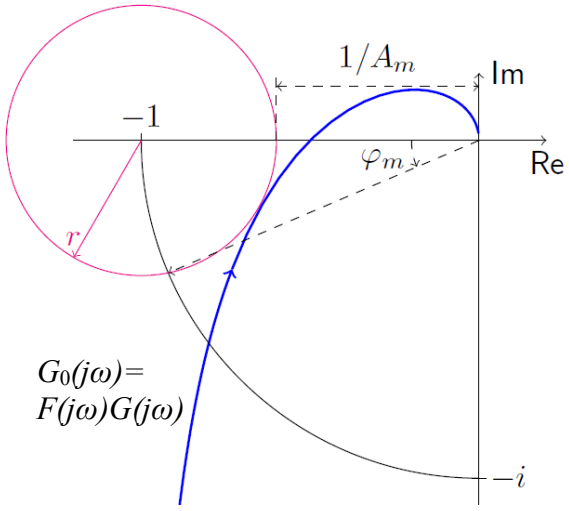

FIGURE 4. NYQUIST DIAGRAM. NOTE THAT THE INDICATED PHASE AND GAIN MARGIN ARE HERE IMPOSED BY THE CIRCLE. THE BLUE CURVE HAS LARGER MARGIN THAN GUARANTEED BY THE EUCLIDIAN DISTANCE.

However, specifying the Euclidian norm guarantees that the amplitude and phase become as follows

$$A_{\mathrm{m}} \geq \frac{1}{1-r} \tag{2.4}$$

$$\boldsymbol{\varphi_{\mathrm{m}} \geq 2\, sin^{-1}(\frac{r}{2})}. \tag{2.5}$$

A drawback with gain and phase margins is the necessity to state both of them in order to guarantee the Nyquist curve not to become close to the critical point. Moreover, phase and amplitude margin, stand-alone or combined, do not guarantee a certain distance to the point -1. Note that none of the mentioned margins guarantee closed loop stability themselves – the point -1 may be encircled without entering the r-circle, and both the unit circle and the negative real axis may be crossed multiple time. However, it can be assumed that the loop gain is simple enough so that such margins ensure stability.

[ii] the factor by which the loop gain can be increased until the Nyquist curve intersects with the point $-1+0\cdot j$

[iii] angle between the negative real axis and the point where the curve crosses a circle centred in origin with unity radius.

Main point: To ensure robust stability it is equivalent to check either the Nyquist curve or the maximum sensitivity (2.6)

The stability margin expressed by the Euclidian norm limits the sensitivity function below a certain value as follows

$$|S(s)| \leq \frac{1}{r} = M_s \tag{2.6}$$

as the sensitivity function is the loop transfer function.

This comes from the fact that the denominator in the sensitivity function is the Euclidian distance between the loop gain and the point -1.

Thus, keep the supremum norm ($max_{\forall\omega}|S(j\omega)|$) below one over r ensures the loop gain not to amplify more at any particular frequency. If nominal stability is fulfilled, i.e. the point -1 in the Nyquist plane is not encircled it implies robust stability and implies uncertainties to be allowed in the plant or controller.

2.2 REJECTION OF DISTURBANCE

The transfer function from a disturbance entering the system is given by

$$\frac{G(s)}{1+G_0(s)} d = S(s)G(s)d = \Delta f \tag{2.7}$$

where Δf is the output of the close loop system.

Thus, the transfer function from a disturbance is the sensitivity function times the transfer function of the system. Therefore, the sensitivity function not only matters in the stability analysis but also plays an important role in how a disturbance propagates in the system. Moreover, the transfer function is independent on the modelling of the disturbance signal - deterministic or stochastic.

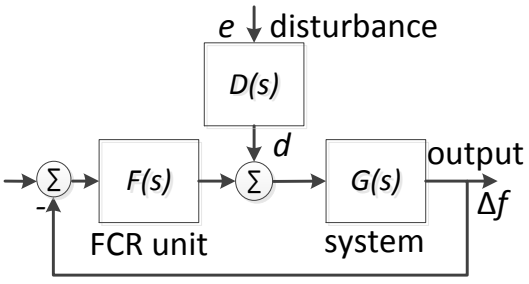

FIGURE 5. OVERVIEW OF THE SYSTEM

Now consider a disturbance, *e(t)*=sin(*ωt*) and |e(*jω*)|=1, that enters the system through a filter *D(s),* shown in Figure 5. Then, assume the control object to be |*Δf(jω)*|<1 for all *ω*. From (2.7) the following can be derived

$$|S(j\omega)| < \frac{1}{[D(j\omega)G(j\omega)]} \tag{2.8}$$

Note that this describes how a signal that enters the system does not propagate in the system so its amplitude is larger than the initial value of the disturbance for any frequency. However, the system is linear and the output is obtained by superposition of the signals that have propagated through the system. If the disturbance signal contains several frequencies, e.g. stochastic signals, they interrelate and may therefore result in input amplitude larger than one even though the power is very low at particular frequencies. Therefore, since the system is linear the output is obtained by superposition. The bottom-line is, the output may therefore also be larger than one. Figure 6 shows a random signal generated by a Gaussian white noise process. White noise has a power spectrum of one and the probability of a random sample to occur outside ±1 is about 32%.

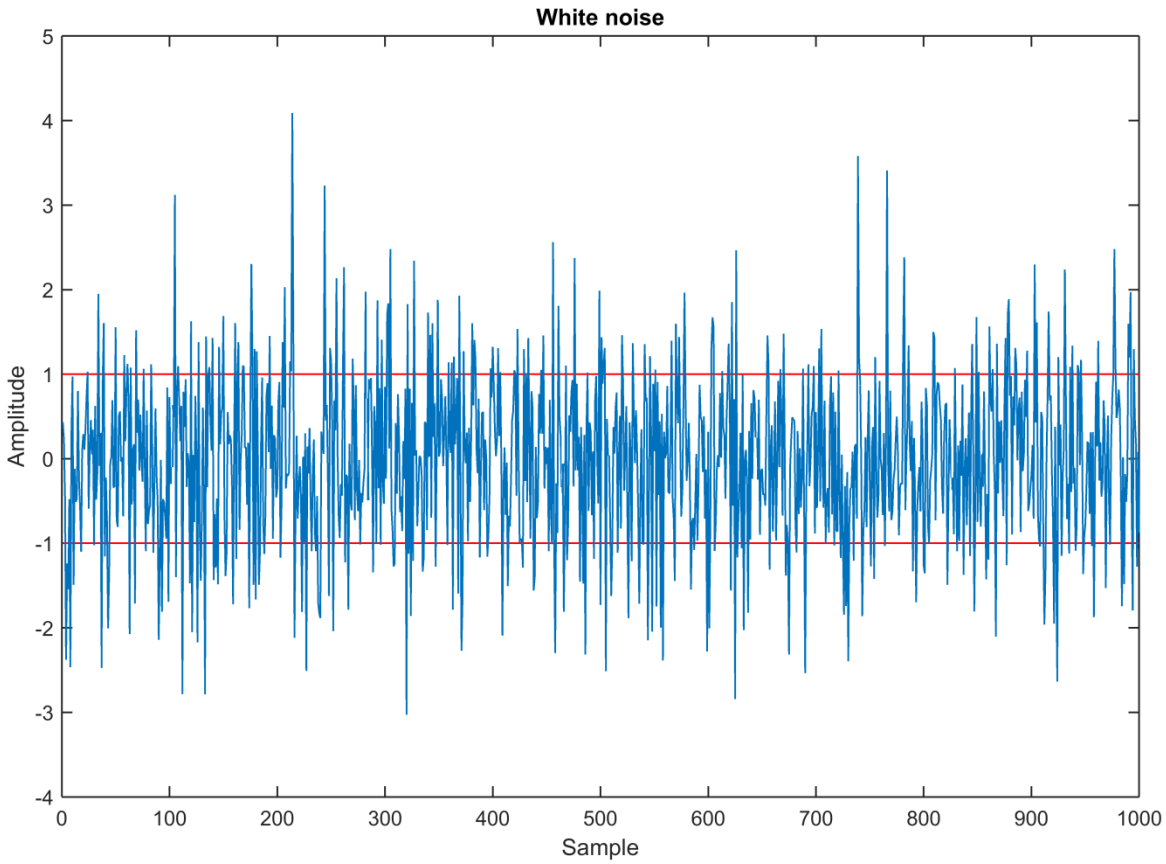

FIGURE 6. STOCHASTIC SIGNAL – WHITE NOISE

3. MODEL DESCRIPTION

This section provides a description of the power system (*G(s)*) and the control unit (*F(s)*) models used. The system consists of generation and consumption distributed in the grid. Thus inertia and

ENTSO-E AISBL • Avenue Cortenbergh 100 • 1000 Brussels • Belgium • Tel +32 2 741 09 50 • Fax +32 2 741 09 51 • info@entsoe.eu • www.entsoe.eu

frequency control is distributed and connected through the grid. In this project, the modelling of the power system and the FCR providing units is performed with the one machine equivalent, assumptions for this are given below.

3.1 POWER SYSTEM MODEL

The swing equation relates the rotor dynamics with mechanical and electrical power of a single machine as

$$\frac{\boldsymbol{H_x}}{\boldsymbol{\pi f_0}}\frac{\boldsymbol{d^2\theta_x}}{\boldsymbol{dt^2}} = \boldsymbol{P_{mx}} - \boldsymbol{P_{ex}} \tag{3.1}$$

where θ_x is the angle in rad of generator *x*, H_x is the inertia constant, P_{mx} and P_{ex} are the mechanical and electrical powers, respectively, expressed on a power base. f_0 is the nominal frequency. Consider the synchronous machines on a common system base (S_n). Assume the machine rotors swing coherently, i.e. all $d\theta_x/dt$ are equal, the powers and the dynamics can then be added as

$$\sum_x \frac{H_x}{\pi f_0}\frac{d^2\theta_x}{dt^2} = \sum_x (P_{mx} - P_{ex}) \tag{3.2}$$

This results in

$$\frac{H}{\pi f_0}\frac{d^2\theta}{dt^2} = P_m - P_e \tag{3.3}$$

where the equivalent inertia constant *H* for the complete system is given by

$$H = \sum H_x \quad \forall x \tag{3.1}$$

where H_x is the inertia constant of generator *x* on this common power base.

Loads are here modelled not to depend on voltage; therefore, they can be lumped. The static loads are assumed to be frequency dependent in proportion to the frequency deviation. Thus, the one mass model together with load frequency dependency then relates the transfer function from power change to frequency change as

$$\Delta f = \frac{f_0}{(2E_\mathrm{k}s + S_\mathrm{n}kf_0)}\Delta P = G(s)\Delta P \tag{3.2}$$

where parameters are specified in Table 2. Thus, this transfer function is a single-input-single-output (SISO) model of the power system. Voltage dependency is not considered as it requires more detailed modelling than the one mass model to properly capture the dynamics. In addition, the view here is that frequency is not strongly correlated with voltage variations.

ENTSO-E AISBL • Avenue Cortenbergh 100 • 1000 Brussels • Belgium • Tel +32 2 741 09 50 • Fax +32 2 741 09 51 • info@entsoe.eu • www.entsoe.eu

3.2 CONTROLLED UNIT

Distributed control implies several controlled units to contribute to the total control work. Figure 7 illustrates several control vectors and the total vector at a particular frequency ω. A unit x provides a response $F_x(j\omega)$ and the total sums to

$$F(j\omega) = \sum_x F_x(j\omega). \quad (3.3)$$

However, here it is assumed that the summed response acts on the coherently swinging system,

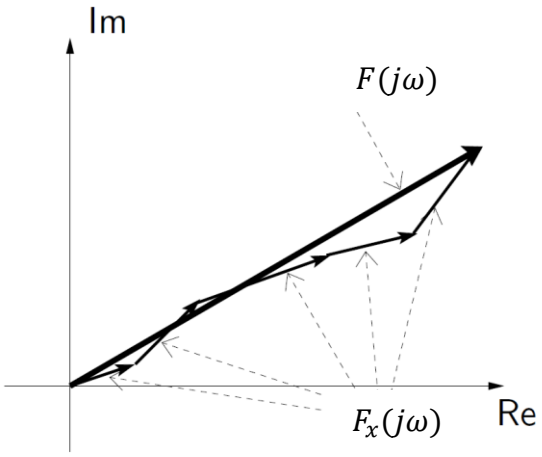

FIGURE 7: TOTAL CONTROL RESPONSE FROM SEVERAL PROVIDERS

explained above. The control response is therefore here assumed to be delivered by a single unit which control response is scaled to correspond to the total regulating strength in the system. Figure 8 shows several units in parallel providing control response to the system.

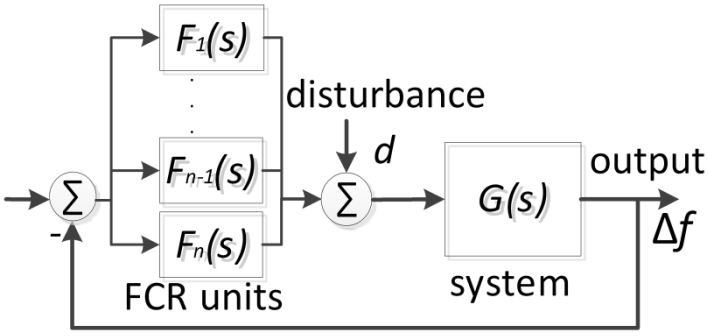

FIGURE 8. OVERVIEW OF SEVERAL FCR-N PROVIDERS IN PARALLEL.

ENTSO-E AISBL • Avenue Cortenbergh 100 • 1000 Brussels • Belgium • Tel +32 2 741 09 50 • Fax +32 2 741 09 51 • info@entsoe.eu • www.entsoe.eu

3.2.1 REFERENCE FCR-UNIT – HYDRO POWER

In this project a simplified hydro power unit is used as a reference unit in order to come up with requirements that also will qualify enough capacity in the Nordic market. The project uses the so called "Nordic frequency model" which is a linear model with backlash on top. An overview of the linear hydro power plant model (F(s)) is displayed in Figure 9. Parameters are defined in Tables 1 and 2. The model is built up of a controller with proportional and integrator part (so called PI-controller), a servo modelled by a low pass-filter in feedback with the droop and the penstock. The penstock provides important and limiting dynamics which are of non-minimum phase. The non-minimum phase dynamic puts limitation on the closed-loop bandwidth but this is not further discussed here.

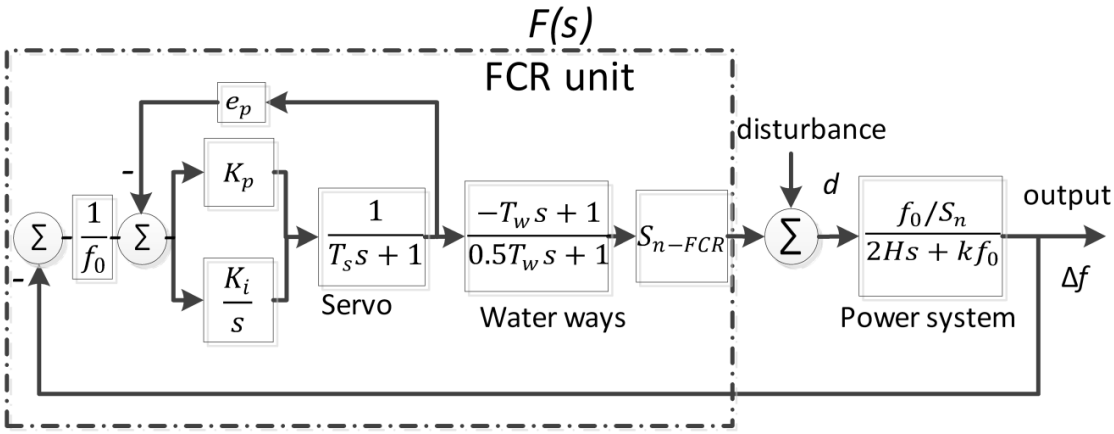

FIGURE 9. LINEAR AGGREGATED REFERENCE MODEL.

The rating and droop value play a role in the provision of FCR, the scaling of individual units' response are explained in Subsection 3.3. Note that the droop value in combination of the power base of the unit defines the regulating strength.

Further details of the hydro power plant modelling can be found in the description of the Nordic frequency Model [2].

Backlash has been added in the model shown in Figure 10 which is added after the servo.

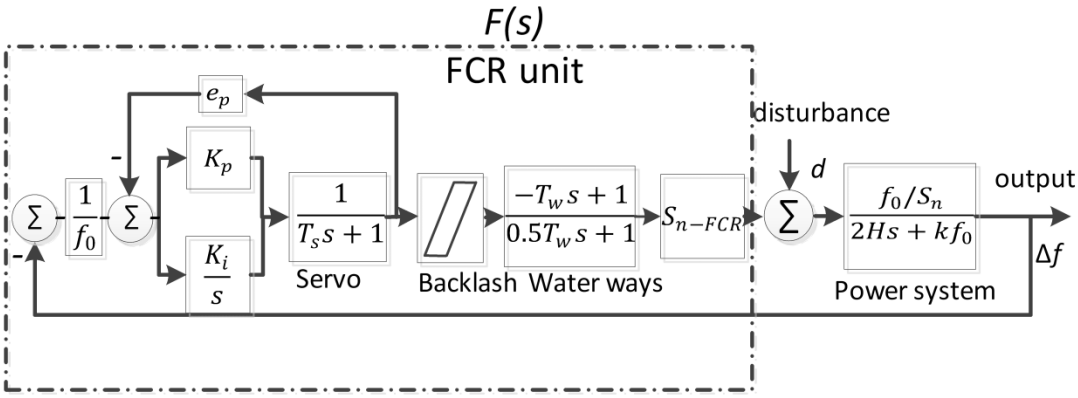

FIGURE 10. NON-LINEAR AGGREGATED REFERENCE MODEL.

The internal feedback can also be by feedback of the power, thus, the backlash is compensated and its impact reduces. The impact from backlash is illustrated in Figure 12 which shows an input signals that passes through a backlash which affects both the phase and amplitude of the output.

Note that we here define backlash as ±b. An input with amplitude A then the output reduces to A-b (if b<A and the backlash centred).

Figure 11 shows the phase shift as function of backlash and is the ratio between the fundamental components of the input and output. Figure 12 provides the phase shift in the time domain and is provided by calculating the fundamental component (through Fast Fourier transform – FFT) of the output signal. Note that only the backlash is considered here, if the input signal passes through an LTI block before it enters the backlash additional phase shift adds up.

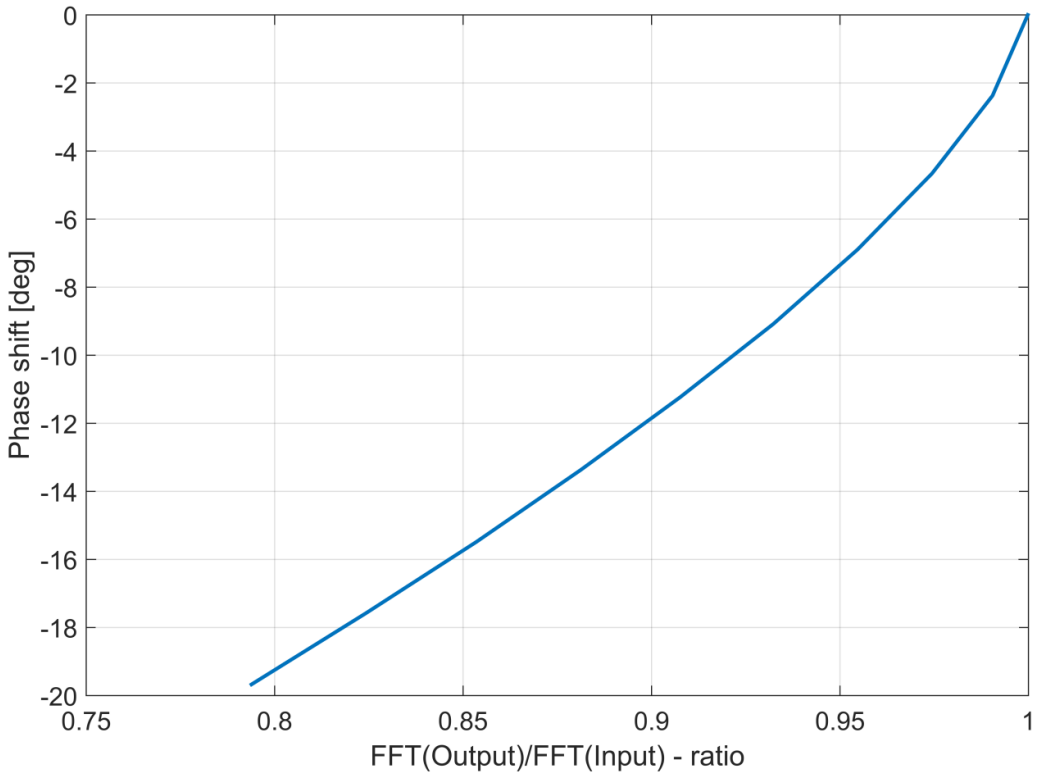

FIGURE 11. PHASE SHIFT AS FUNCTION OF THE RATIO BETWEEN THE BACKLASH AND SIGNAL AMPLITUDE.

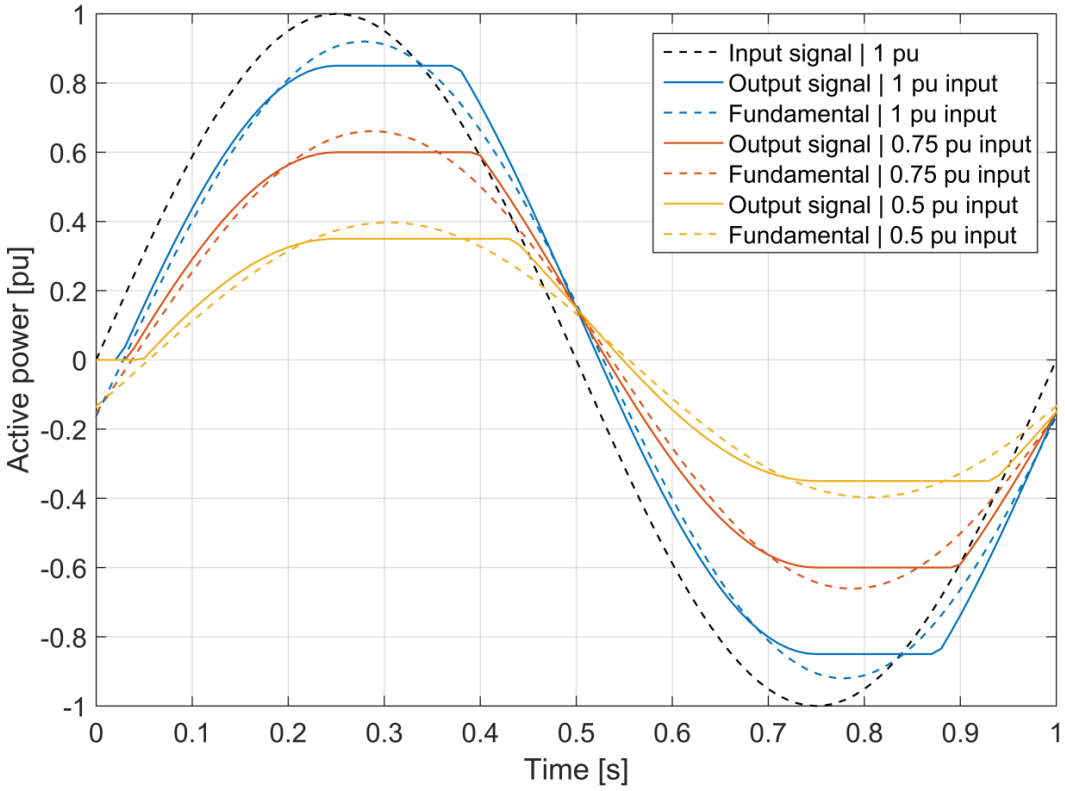

FIGURE 12. PHASE SHIFT FOR DIFFERENT BACKLASH VALUES

Applying the Fast Fourier transform (FFT) of a sinusoidal signal with amplitude A results in an amplitude of A at the particular frequency of the sinusoidal. However, the FFT of the output signal with backlash results in an amplitude larger than A-b. Thus, the impact of backlash is indirectly reflected in linear analysis as it is included in the output response. The fundamental component scaling takes into account the fact that the amplitude of the fundamental component is larger than the actual signal, as shown in Figure 13.

ENTSO-E AISBL • Avenue Cortenbergh 100 • 1000 Brussels • Belgium • Tel +32 2 741 09 50 • Fax +32 2 741 09 51 • info@entsoe.eu • www.entsoe.eu

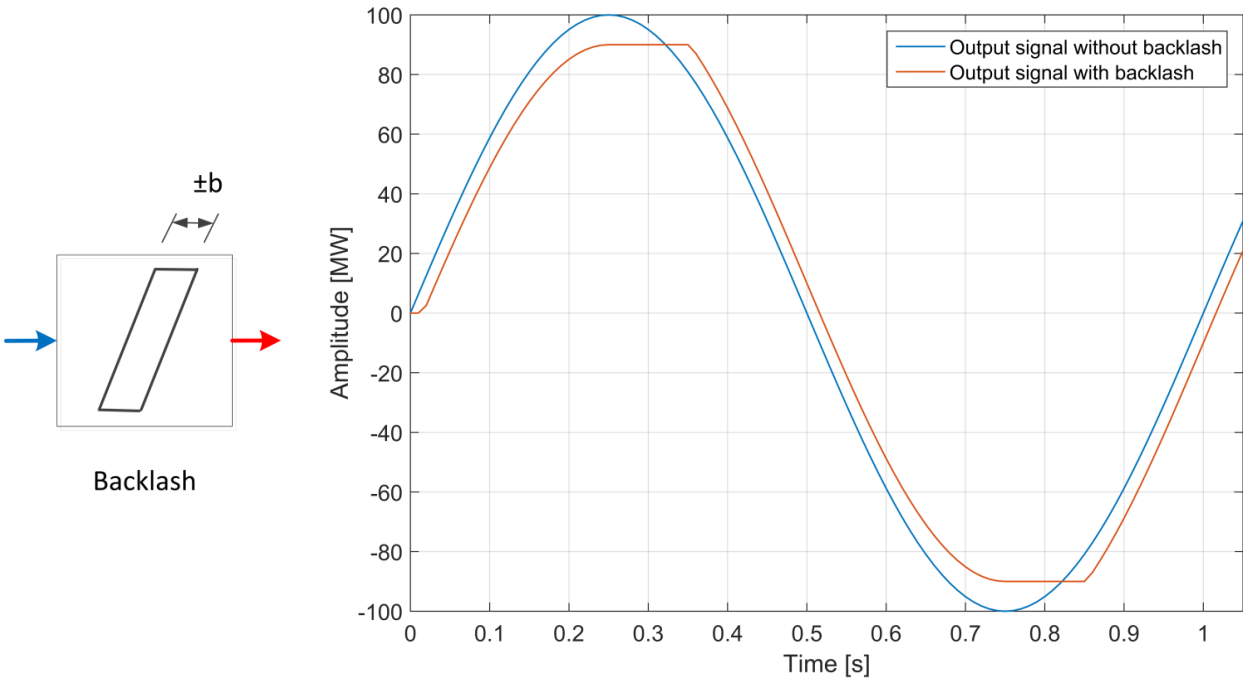

FIGURE 13. INFLUENCE OF BACKLASH ON A SINUSOIDAL SIGNAL.

The calculation of the fundamental scaling factor, α, is done based on the size of the backlash in relation to the signal strength. In a block diagram in Figure 14 the calculation is shown. In the sine-in-sine-out tests the unit is trying to provide a signal $a(t)$ but due to the backlash the signal will not be purely sinusoidal. The signal $y(t)$ represents the output signal due to backlash. Signals a(t) and y(t) are the blue and red curves in Figure 13, respectively. $a(t)$ is given as

$$a(t) = \sin(\omega_0 t) \tag{3.4}$$

where $\omega_0$is an arbitrary frequency > 0.

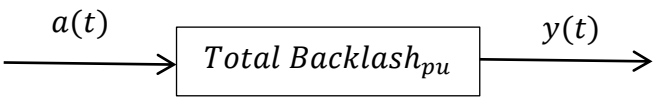

FIGURE 14. BLOCK DIAGRAM OF THE TOTAL BACKLASH

Now the output signal $y(t)$ can be simulated with *a(t)* entering the backlash block, shown in Figure 14. The discrete FFT is calculated of the input and output signals as

$$A(k) = \sum_{0}^{N-1} a(n)\, e^{\frac{-j2\pi nk}{N}} \tag{3.5}$$

$$\boldsymbol{Y(k) = \sum_{0}^{N-1} y(n)\, e^{\frac{-j2\pi nk}{N}}} \tag{3.6}$$

The fundamental scaling factor can be calculated after performing the Fourier transforms.

$$\alpha = \frac{Y(\omega_0)}{A(\omega_0)} \tag{3.7}$$

Table 3 shows different backlash values and the corresponding scaling factor, α.

TABLE 3. BACKLASH SCALING FACTOR (α) AS A FUNCTION OF TOTAL BACKLASH IN PERCENT OF TOTAL SIGNAL STRENGTH ($\pm b$)

$2b$	0 %	1 %	2 %	3 %	4 %	5 %	6 %
α	1	0.999	0.998	0.997	0.996	0.994	0.992
$2b$	7 %	8 %	9 %	10 %	11 %	12 %	13 %
α	0.99	0.988	0.986	0.984	0.981	0.979	0.976
$2b$	14 %	15 %	16 %	17 %	18 %	19 %	20 %
α	0.974	0.971	0.968	0.965	0.962	0.959	0.956
$2b$	21 %	22 %	23 %	24 %	25 %	26 %	27 %
α	0.953	0.95	0.946	0.943	0.94	0.936	0.932
$2b$	28 %	29 %	30 %				
α	0.929	0.925	0.921				

The internal feedback, e_p, in an FCR-unit is most often expressed in percentage and is called droop. This percentage value is expressed on its own power base, most often rated power, and is defined as

$$e_p = \frac{{}^{df}/_{f_0}}{{}^{\Delta P}/_{S_{\mathrm{n}-FCR}}}. \tag{3.8}$$

This equation states, a unit changes its power by 100 % at frequency change of e_p [%]. Example, a unit with droop of 6 % requires the frequency to drop $0.06 \cdot 50\ Hz = 3\ Hz$ to change its power by 100 %. Droops are commonly in the range 2-12% which implies the power change for FCR-N (±0.1 Hz) is in the range of ±10 % to ±1.67 % of the machines' power base.

Backlash reduces the output and a typical backlash value of hydro power plants in the Nordic system is around ±0.005 pu[iv] [3]. Note that this value is given on the power base of the machine and is independent of the droop. However, the ratio backlash divided by FCR-N capacity is strongly depended on the droop. In order to achieve the required total steady-state capacity backlash is compensated according to

$$\Delta P_{\mathrm{FCR}} = S_{\mathrm{n-FCR}} \left[\frac{df}{f_0} \cdot \frac{1}{e_\mathrm{p}} - b \right] \tag{3.9}$$

[iv] Based on the machine's power base

where $\Delta P_{\mathrm{FCR}}$is the FCR capacity.

3.3 PER UNIT SCALING

Until now physical units have been used for the system input and output. These physical inputs and outputs can be scaled to per unit (pu). For the FCR-N three different per unit scaling have been used, these are

1. Per unit – droop base

   Scaling is based on the droop value and scales the rated power (or number of machines) to deliver 600 MW FCR-N in total – Used in the simulation study.

2. A. Per unit – FCR-N capacity base

   Scaling is based on FCR-N delivery, the power and frequency deviation bases are 600 MW and 0.1 Hz, respectively – Used in the control design.

   B. Per unit – machine base

   Scaling is based on the capacity delivered from an individual unit. The power base comes from the frequency step responses where the static gain is equal to one per unit – Used in the actual testing.

Hence, it is important to know on which base the per unit values refers to as they may seem to be similar. The beauty with per unit is that individual units' responses are scaled to one whereas the system also scales to one which then makes them compatible without further scaling. More detailed description is given below.

3.3.1 PER UNIT SCALING – DROOP BASED

This per unit scaling uses given droop values as the base to derive the power base. For this, there are now two options, the power base of a single machine is scaled to deliver the full capacity of FCR-N based on the selected droop or the machine power base is also chosen and the number of machines is scaled to deliver the right amount of FCR-N.

The rated power of a single FCR unit delivering the capacity dP with a droop of e_p corresponds to

$$S_{\mathrm{n-FCR}} = e_{\mathrm{P}} \cdot dP \cdot \frac{f_0}{df}. \tag{3.10}$$

The capacity of 600 MW using droop $\boldsymbol{e_p}$ =6 % gives the rated power as

$$S_{\mathrm{n-FCR6\%}} = e_{\mathrm{P}} \cdot dP \cdot \frac{f_0}{df} = 0.06 \cdot 600 \cdot \frac{50\mathrm{Hz}}{0.1\mathrm{Hz}}\mathrm{MVA} = 18\,000\ \mathrm{MVA}. \tag{3.11}$$

Alternatively, each unit on the base $S_{\text{n-FCR}}$, using droop of 6 %, delivers a capacity of

$$\Delta P = S_{\mathrm{N-FCR}} \cdot \frac{df}{f_0} \cdot \frac{1}{e_{\mathrm{P}}} \tag{3.12}$$

with similar numbers as above each unit delivers

$$\Delta P = S_{\mathrm{N-FCR}} \cdot \frac{df}{f_0} \cdot \frac{1}{e_{\mathrm{P}}} = 600 \cdot \frac{0.1}{50} \cdot \frac{1}{0.06} = 20\ \mathrm{MW}. \tag{3.13}$$

To deliver the full amount, *n* number of units is required which calculates as

$$n = \frac{dP}{\Delta P}. \tag{3.14}$$

Simulation runs performed in the Nordic frequency model are based on this per unit scaling. Since the model, backlash excluded, is linear one single machine can be used to provide the whole capacity.

3.3.2 A. PER UNIT SCALING ON SYSTEM LEVEL

The SISO-model in Figure 15 has physical units for input/output (I/O). By defining the power base as

$$dP = 600\ MVA = 1\ pu \tag{3.15}$$

and the frequency deviation base as

$$df = 0.1\ Hz = 1\ pu. \tag{3.16}$$

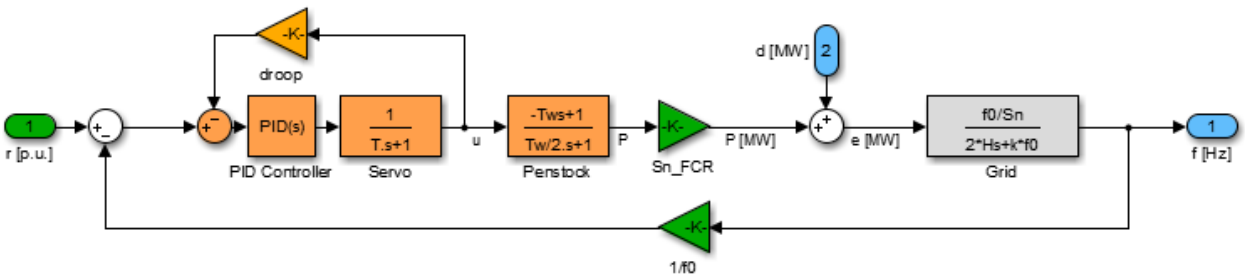

FIGURE 15. A (SISO) FREQUENCY CONTROL MODEL. SEE TABLE 1 FOR VARIABLE DEFINITION.

The input and output static gain for the FCR-provider becomes one per unit. This step of the scaling can be achieved since the droop e_p is defined as

$$e_{\mathrm{p}} = \frac{{}^{\mathrm{d}f}/_{f_0}}{{}^{dP}/_{S_{\mathrm{n-FCR}}}} \tag{3.17}$$

where df and f_0 are the frequency deviation limit and nominal frequency, respectively. dP is the static capacity of the unit and $S_{\mathrm{N-FCR}}$ the rated power of the unit.

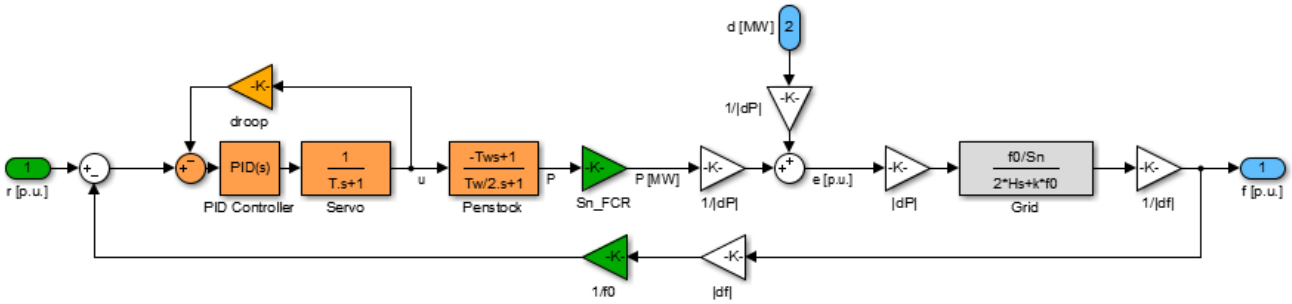

FIGURE 16. SISO-MODEL IN FIGURE 15 SCALED FROM PHYSICAL UNITS TO PU I/O

Then the system scales to

$$G(s) = \frac{dP \cdot \frac{f_0}{df}}{2E_{\mathrm{k}}s + kf_0S_n}, \tag{3.18}$$

The response from an FCR-unit is one per unit with droop of 0.002 (0.2 %) and rated power 600 MVA. This simplification of the modelling is shown in Figure 17.

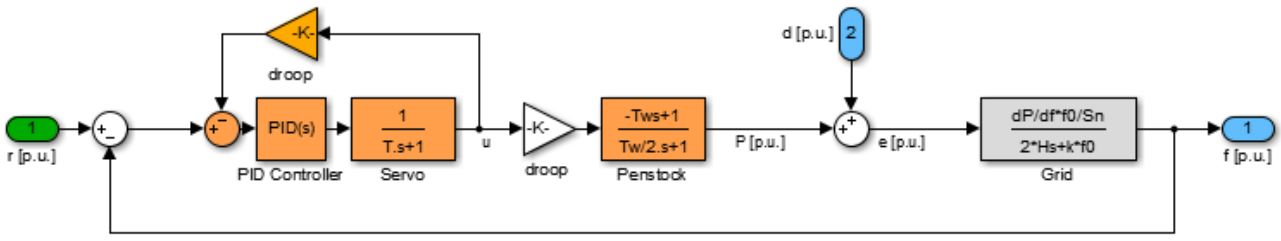

FIGURE 17. SIMPLIFICATION OF SCALED MODEL IN FIGURE 16.

3.3.3 B. PER UNIT SCALING – MACHINE BASE

The normalization is defined so that the static gain of an FCR unit shall be equal to one per unit, i.e.

$$FFT[F(j\omega)] = 1\ \mathrm{pu} \quad \omega \to 0. \tag{3.19}$$

Such scaling is performed by incorporating the backlash and the fundamental component of the output signal. Further description is given in Section 5.

4. DESIGN OF REQUIREMENTS

The goals of the design are to improve the frequency quality and to ensure stability. The main measure of frequency quality is minutes outside normal band (MoNB) – mathematically defined as

$$kpi_{MoNB} = \frac{\begin{cases} \int dt, & |\Delta f(t)| > 0.1\ Hz \\ 0, & |\Delta f(t)| < 0.1\ Hz \end{cases}}{\int dt}. \tag{4.1}$$

This KPI is mentioned in the constraints and specifies that MoNB should be less than 10 000 minutes per year corresponding to 1.9 % of the time.

The methodology developed within this project, for creating the future requirements imposed on the FCR-N, is based on linear design considering fundamental limitations [4]. Stability and performance are expressed with and without uncertainty as

- *Nominal stability*: The system is stable with no model/control uncertainty
- *Nominal performance*: The system satisfies the performance specifications with no model/control uncertainty
- *Robust stability*: The system is stable for all perturbed plants/controller about the nominal model up to the worst-case model uncertainty.
- *Robust performance*: The system satisfies the performance specifications for all perturbed plants/controllers about the nominal model up to the worst-case model uncertainty.

The project applies robust stability for the low inertia system in addition to low frequency dependency of loads. This implies an uncertainty for the low inertia system, given by the Euclidian distance, is allowed before instability. Thus, there is an uncertainty margin which can either be in the plant or in the FCR-unit response. This can be realised from the Nyquist curve as the loop gain is defined by the system response times the controller response.

Moreover, the project has chosen to use nominal performance which means performance meets the requirements in the average inertia system without uncertainty and provides acceptable frequency quality on average. However, it is likely that the power disturbance varies over the year but not necessarily correlated with the variation in the inertia of the system.

Hence, stability is expressed on the low inertia system and performance is expressed on the average inertia system. The project believes that by using nominal performance and robust stability a significant policy step forward is made compared to the current situation in the Nordic synchronous area. In the future, an enhancement of this policy would be to move from nominal performance towards robust performance.

ENTSO-E AISBL • Avenue Cortenbergh 100 • 1000 Brussels • Belgium • Tel +32 2 741 09 50 • Fax +32 2 741 09 51 • info@entsoe.eu • www.entsoe.eu

4.1 STABILITY REQUIREMENT

The constraints, see Section 1, specify minimum stability requirements in terms of phase margin. Using this margin the maximum sensitivity M_s is calculated from (2.6) as

$$M_s = \frac{1}{r} = \frac{1}{2\cdot\sin(\frac{\varphi_m}{2}\cdot\frac{\pi}{180})} = \frac{1}{2*\sin(\frac{25}{2}*\frac{\pi}{180})} = 2.31. \quad (4.2)$$

Thus, a circle with radius $1/M_s$ is plotted in the Nyquist diagram centred at the point -1. For accepted control response, i.e. robust stability, the Nyquist curve shall not enter the circle or encircle the point -1. However, so far the response is on the complete FCR response and not on unit level. This can also be expressed as a requirement on the sensitivity function as

$$\boxed{|S_{\min}(s)|_{\forall\omega} < M_s = 2.31} \quad (4.3)$$

where $S_{min}(s)$ expresses the low inertia system. Scaling to individual units is explained in Section 5.

Example:

To exemplify the robustness, study the margin for the increased regulating strength. Stability requires the point -1 to not be encircled. Therefore, consider the loop point that has 180° phase shift ($F(j\omega_1)\cdot G(j\omega_1)=-1$) pointing in the negative direction along the real axis. Assume the point to lie just at the circle, i.e. the coordinate is 0j+(r-1). Then, the loop gain is written as a function of the regulating strength as follows

$$G_0|_{\omega 1} = F(j\omega_1)G(j\omega_1) = \frac{(R_0+\Delta R)}{6000}(1-r)e^{j\pi} \quad (4.4)$$

where R_0=6000 MW/Hz is the regulating strength used in the design and ΔR is the additional regulating strength.

This corresponds to scale the regulating strength as follows

$$\frac{(6000+\Delta R)}{6000}(1-r)e^{j\pi} > -1 \quad (4.5)$$

Then, $\Delta R < 4582$ MW/Hz

Note that the frequency will oscillate and the quality may be poor but stability is ensured. Additional regulating strength coming from backlash is not included. Since the capacity is reduced from backlash the regulating strength in terms of MW per Hz will increase as backlash comes in to play. This is explained by the fact that the procured capacity is the steady state capacity.

4.2 PERFORMANCE REQUIREMENT

To develop performance requirements the disturbance needs to be quantified. The disturbance is here net-power variations in normal operation that are to be balanced by the FCR-N. This variation was estimated by accessing the energy metering system that Svenska kraftnät operates. Within this energy metering system, all transfers between the grid owned by Svenska kraftnät and a third party are monitored and logged with sufficient accuracy and with a sampling rate of three seconds. The system also includes energy meters for all tie-lines connecting between different

bidding areas within Sweden. The tie-lines used to measure the net imbalances of a larger area were the AC tie-lines interconnecting Areas SE3 and SE4, see Figure 18. This area was measured because there is a very small amount of FCR-N active within this area, giving the measured values a high degree of relevancy for the underlying stochastic generation-load imbalances. Also, the load within the southern Swedish area constitutes on average a third of the total load in the Nordic system. The data processing and detailed results are provided by the Imbalance study, see [5].

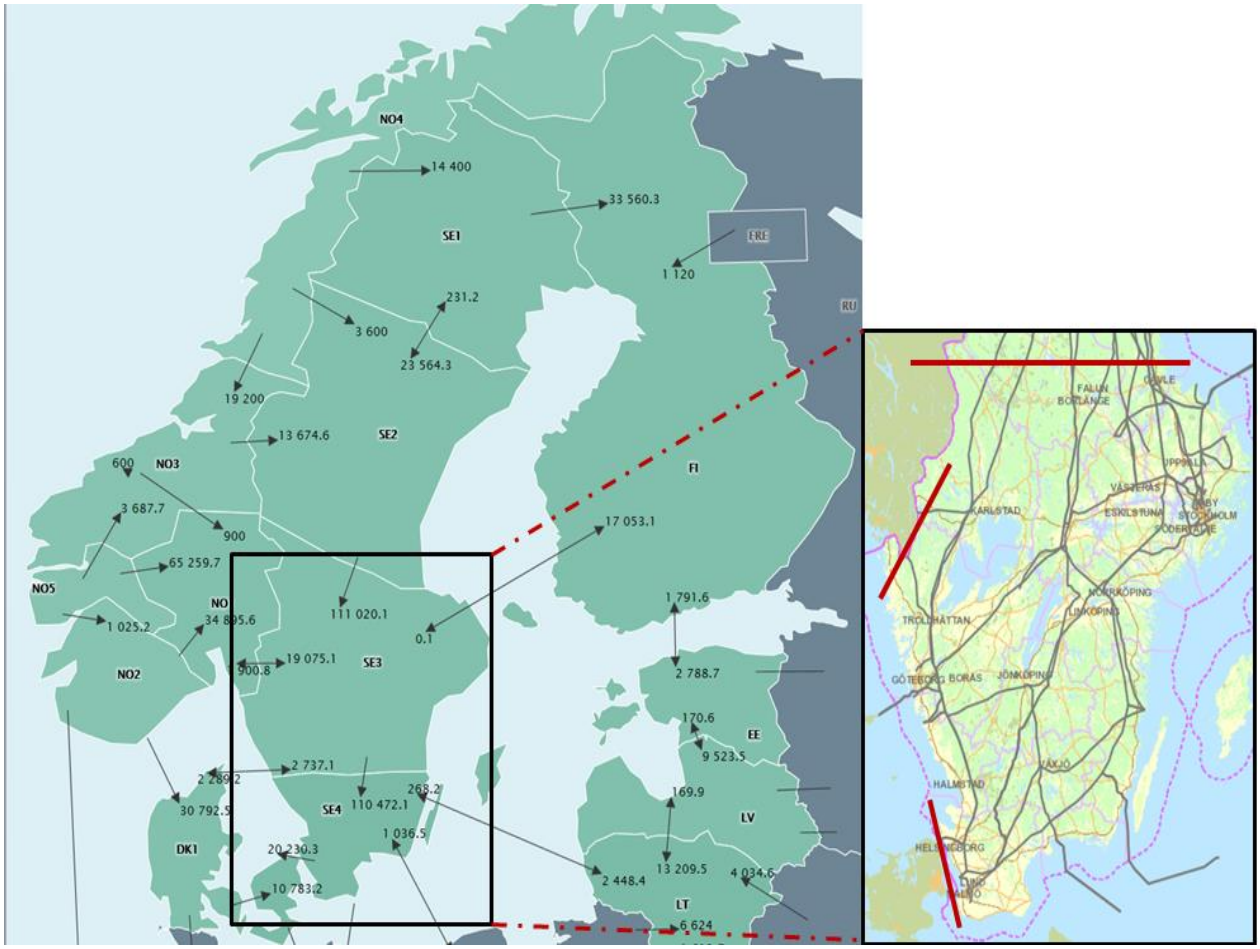

FIGURE 18. SCHEMATIC DESCRIPTION OF WHICH TIE-LINES MEASURED TO ESTIMATE GENERATION-LOAD IMBALANCES. MEASURED CUTS ARE THOSE SHOWN WITH A RED LINE IN THE MAP ON RIGHT HAND SIDE.

The study aimed to emulate the statistical properties of the measured net-variation by modelling it as the output of a linear filter with white noise as input. The study estimated the variations to have low-pass characteristics and the process is given by

$$d = D_{\text{est}}(s)w = \frac{\sqrt{3}\cdot 12}{s}w \tag{4.6}$$

where *d* is the net-power variation and *w* is the white noise input to the filter $D_{est}(s)$. The aFRR also contributes to balance the system and with its integration balancing from 2-3 minutes in addition to the tertiary frequency control, manual frequency restoration reserve. In steady-state the capacity is specified to 600 MW and therefore the imbalance profile is mapped to a first order filter as

$$D(s) = \frac{600}{T_{\text{dist}}s + 1} \tag{4.7}$$

where T_{dist} is the time constant of the imbalance profile.

Measurement data were not available over longer periods to estimate net-power variations in order to verify the spread.

Eq. (2.7) states how a disturbance propagates through the system and is now written as

$$S_{\text{avg}}(s)D(s)G_{\text{avg}}(s)w = f \tag{4.8}$$

where $G_{avg}(s)$ is the transfer function of the average inertia system. Rewriting this as

$$S_{\text{avg}}(s)w = \frac{1}{D(s)G_{\text{avg}}(s)}f. \tag{4.9}$$

The power spectral density (PSD) state the relation between the input signal and the output given as

$$\left|S_{\text{avg}}(j\omega)\right|^2 \emptyset_w(j\omega) = \frac{1}{|D(j\omega)G_{\text{avg}}(j\omega)|^2}\emptyset_{\text{f}}(j\omega) \tag{4.10}$$

where $\emptyset_{\text{w}}(j\omega)$ is white noise with PSD equal to one and $\emptyset_{\text{f}}(j\omega)$ is the PSD of the frequency deviation.

An output with equal limitation at each frequency and the PSD is constant $\emptyset_{\text{f}}(j\omega) = \sigma_{\text{f}}^2$ is required.

This choice specifies a boundary of the amplification of all frequencies and a variance of the frequency deviation. The **performance requirement** then becomes

$$\boxed{\left|S_{avg}(s)\right| < \frac{\sigma_{\text{f}}}{|D(s)G_{\text{avg}}(s)|} = \sigma_f \frac{|T_{\text{dist}}s+1|}{D(j0)|G_{\text{avg}}(s)|}}. \tag{4.11}$$

From this, the steady-state value is 6000 MW/Hz which is the ratio between σ_f and *D(j0).* As mentioned before, deterministic disturbance signals require that (4.11) is fulfilled (with $\sigma_{\text{f}} = 0.1$) in order to let an input signal of amplitude 600·sin(ωt) MW (=1 pu) not result in a frequency deviation larger than 0.1·sin(ωt) Hz (=1 pu).

Enforcing the frequency target to 0.1 Hz/Hz at all frequencies and select the time constant to align the transfer function in (4.11) does not necessarily ensure the frequency within ±0.1 Hz. As argued above, stochastic signals are better described by the statistical property. If the output frequency has the characteristics of white noise the frequency target have to be significantly reduced. Fortunately this is not the case as the bandwidth of the output is bounded since the inertia of the system reduces the effect on the output at high frequencies - what matter is the variance of the output frequency.. The power spectrum does not necessary have to be smaller than 0.1 Hz/Hz for all frequencies as it appears smaller at other frequencies.

In order to match the disturbance spectrum, and to still be able to obtain acceptable frequency quality, an appropriate time constant must be found. The filter constant is found through analysis

of a huge amount of simulation runs with various parameters sweeps that were performed in the Nordic frequency model.

In order to reduce the quadratic sum of the frequency deviation, which relates to variance of the output frequency, the approach above is not most appropriate. However, the approach specified above has advantage when it comes to real testing and implementation as it is straightforward to put requirement at particular time periods. Also, linear optimisation, see Appendix B, was performed to find parameters (K_p and K_i) for the linear reference unit that fulfilled the requirements. It was shown that there is a correlation between the resonance peak of the sensitivity function and frequency quality. This peak is directly related to the stability margin.

The imbalance study indicated that the disturbance could be mapped to a low pass filter. There is a trade-off between the filter constant and frequency quality while harder requirements result in less capacity on the market. The simulations are performed with the Nordic frequency model-profile by parameter sweeps over, K_p, T_i, backlash and droop. Then the minutes outside normal band, described in next subsection, are quantified.

4.3 REQUIREMENTS

There are several aspects to consider when deciding the filter constant of the disturbance filter. As described earlier, backlash has a great impact on the stability and performance. Thus, the signal strength plays an important role and there is a trade-off between this and the filter time constant.

Figure 19 illustrates an example of the sensitivity functions for specific parameters of the linear hydro power model.

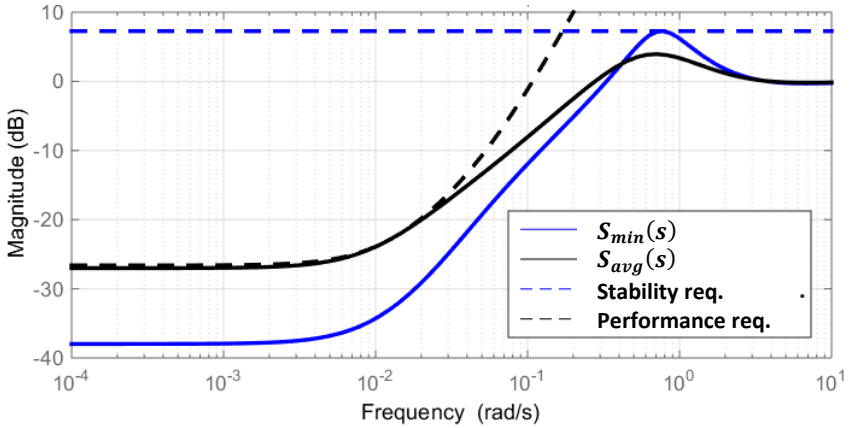

FIGURE 19. ILLUSTRATION OF REQUIREMENTS AND PLOTTED SENSITIVITY FUNCTIONS

Note that, inspection of Figure 19 clearly shows typical margins between the sensitivity function of the low inertia system and the performance requirement. The low inertia system, instead, is limited by the stability requirement. Note that, the performance requirement is here plotted based on the average inertia system. The slope in the performance curve is moved to the right with decreased inertia.

To create a picture of the trade-off, a huge amount of simulations were performed. Figure 19 indicates that the performance requirement is close to be violated around $\omega=10^{-2}$ rad/s and the

stability requirement around $\omega=6\cdot10^{-1}$ rad/s. Thus, performance is the limiting factor at longer time periods (≈600-200 s) and stability at shorter time periods (≈60-10 s).

In the beginning of the project 30 mHz was proposed for testing, with time it turned out backlash had too much impact compared to the units' response.

Since the signal strength has great impact it has to be coordinated in order to find reasonable over-all requirements. It turned out that impact on the performance from backlash occurred at longer time periods where the phase lag of the FCR-response still was low. The backlash is more or less fixed as it comes from mechanical parts and is here specified in per unit, as described earlier. From the tests performed with 50 mHz amplitude it was seen that it is only possible to fulfil the requirements for backlash up to ±0.004 pu, shown in Table 4. As set of parameters is a combination of Kp and Ki, the range of the parameters simulated in Table 4 is

K_i=[0.1, 0.15, 0.2, 0.25, 0.3, 0.4]

and

K_p=[1, 1.5, 2, 2.5, 3, 3.5, 4, 4.5, 5, 5.5, 6, 6.5, 7, 7.5, 8, 8.5, 9, 9.5, 10]

which leads to 72 combinations. In addition to this, a sweep is run over backlash and droop. In total 4752 number of qualification runs were performed.

ENTSO-E AISBL • Avenue Cortenbergh 100 • 1000 Brussels • Belgium • Tel +32 2 741 09 50 • Fax +32 2 741 09 51 • info@entsoe.eu • www.entsoe.eu

TABLE 4. NUMBER OF QUALIFIED PARAMETER SETS (MAXIMUM 72) AS TIME CONSTANT OF THE DISTURBANCE FILTER VARIES BETWEEN 70 S – 100 S.

70 s

Droop\BL	0	0,001	0,002	0,003	0,004	0,005	0,006	0,007	0,008	0,009	0,01
2%	36	36	36	32	20	0	0	0	0	0	0
4%	36	36	22	14	4	0	0	0	0	0	0
6%	36	27	11	1	0	0	0	0	0	0	0
8%	36	19	3	0	0	0	0	0	0	0	0
10%	36	15	0	0	0	0	0	0	0	0	0
12%	36	11	0	0	0	0	0	0	0	0	0

80 s

Droop\BL	0	0,001	0,002	0,003	0,004	0,005	0,006	0,007	0,008	0,009	0,01
2%	48	38	36	33	30	0	0	0	0	0	0
4%	40	36	30	22	9	0	0	0	0	0	0
6%	42	28	19	1	0	0	0	0	0	0	0
8%	42	26	6	0	0	0	0	0	0	0	0
10%	42	23	0	0	0	0	0	0	0	0	0
12%	42	19	0	0	0	0	0	0	0	0	0

90 s

Droop\BL	0	0,001	0,002	0,003	0,004	0,005	0,006	0,007	0,008	0,009	0,01
2%	48	48	48	44	30	0	0	0	0	0	0
4%	48	48	40	22	10	0	0	0	0	0	0
6%	48	39	19	3	0	0	0	0	0	0	0
8%	48	35	8	0	0	0	0	0	0	0	0
10%	48	24	0	0	0	0	0	0	0	0	0
12%	48	19	0	0	0	0	0	0	0	0	0

100 s

Droop\BL	0	0,001	0,002	0,003	0,004	0,005	0,006	0,007	0,008	0,009	0,01
2%	48	48	48	45	41	0	0	0	0	0	0
4%	52	48	41	30	10	0	0	0	0	0	0
6%	52	40	27	3	0	0	0	0	0	0	0
8%	52	36	9	0	0	0	0	0	0	0	0
10%	52	32	0	0	0	0	0	0	0	0	0
12%	52	27	0	0	0	0	0	0	0	0	0

One can argue, if the backlash is ±10 % for an input amplitude of ±100 mHz, i.e. the maximum output is 90 %. Then if reducing the input amplitude to ±50 mHz, the maximum output becomes 80 %. Clearly, the loss in amplitude has increased by a factor of two. Supported by this argument, and the fact that only a low value of the backlash was allowed, an amplitude of ±100 mHz was chosen for performance[v] requirements to reduce the impact from the backlash.

The impact from backlash on the stability requirement is more complex as both the amplitude and phase lag are reduced at the time periods of interest. A first attempt was to use amplitude of 50 mHz. This in order to capture instability in the range of small variation of the input which is the normal variation of today in the Nordic power system.

In order to decide a proper time constant for performance another round of simulations were performed on the Nordic frequency model. The results when varying backlash and droop are

[v] Also for stability – motivated by the fact that it will make the actual testing simpler without affecting the results too much.

shown in Table 7 and Table 8 for variation of the droop. These were then compared to each other together with the MoNB. The parameter sweeps are shown in Table 5 where the number of combinations are 19·10·12·6=13680. The parameters that are sweeped are K_p, T_i, droop and backlash. These are sweeped for each choice of performance time constant i.e. 50-90 s. Table 6 shows the percentage of qualified units' parameters and Figure 20 shows the duration curve with 600 MW FCR-N for different time constants. The x-axis indicates the percentage of all qualified units producing MoNB that is lower than or equal to a certain value (y-axis). Based on all simulations and studying the MoNB the time constant was selected to 70 s.

Note that T_i is here defined as

$$T_i = \frac{1}{e_p K_i}. \tag{4.12}$$

The control structure used in the models has K_i implemented, see Figure 9. In the simulations K_i is scaled with e_p so T_i becomes the same for any droop. The base case used is with a droop of 6 %.

TABLE 5. PARAMETER RANGES USED IN THE SIMULATION STUDY.

Parameter	Step size	Interval
K_p	0.5	1-10
T_i	10 s	10-100 s
Droop	2%	2-12%
Backlash	0.001 pu	0-0.012 pu

TABLE 6. SHARE OF COMBINATIONS THAT QUALIFY

Time constant	Share that qualified
50 s	6.32%
60 s	9.81%
70 s	13.45%
80 s	17.18%
90 s	20.30%

TABLE 7. NUMBER OF COMBINATIONS (MAXIMUM 100) QUALIFIED FOR PERFORMANCE AND STABILITY.

50 s													
Droop\BL	0	0,001	0,002	0,003	0,004	0,005	0,006	0,007	0,008	0,009	0,01	0,011	0,012
2%	20	16	11	9	7	4	2	1	0	0	0	0	0
4%	30	24	20	17	14	9	6	4	1	0	0	0	0
6%	32	23	12	8	6	2	0	0	0	0	0	0	0
8%	37	22	8	6	1	0	0	0	0	0	0	0	0
10%	41	21	4	3	1	0	0	0	0	0	0	0	0
12%	45	22	4	0	0	0	0	0	0	0	0	0	0

60 s													
Droop\BL	0	0,001	0,002	0,003	0,004	0,005	0,006	0,007	0,008	0,009	0,01	0,011	0,012
2%	29	25	21	15	12	9	6	4	2	1	0	0	0
4%	41	36	28	24	20	14	10	6	3	0	0	0	0
6%	44	35	18	12	11	5	2	0	0	0	0	0	0
8%	51	35	12	9	2	1	0	0	0	0	0	0	0
10%	59	36	6	4	2	0	0	0	0	0	0	0	0
12%	69	39	6	1	0	0	0	0	0	0	0	0	0

70 s													
Droop\BL	0	0,001	0,002	0,003	0,004	0,005	0,006	0,007	0,008	0,009	0,01	0,011	0,012
2%	38	34	29	24	20	13	10	7	4	2	0	0	0
4%	50	45	39	32	26	20	16	9	6	2	1	0	0
6%	56	50	25	16	16	7	5	2	0	0	0	0	0
8%	68	51	16	13	5	3	0	0	0	0	0	0	0
10%	76	52	8	6	4	0	0	0	0	0	0	0	0
12%	80	51	9	3	0	0	0	0	0	0	0	0	0

80 s													
Droop\BL	0	0,001	0,002	0,003	0,004	0,005	0,006	0,007	0,008	0,009	0,01	0,011	0,012
2%	48	42	37	31	28	19	15	11	7	4	1	0	0
4%	61	55	52	41	33	26	20	14	10	4	2	0	0
6%	72	63	33	23	21	14	8	3	1	0	0	0	0
8%	81	66	21	17	9	5	2	0	0	0	0	0	0
10%	86	64	11	10	6	0	0	0	0	0	0	0	0
12%	88	57	12	5	1	0	0	0	0	0	0	0	0

90 s													
Droop\BL	0	0,001	0,002	0,003	0,004	0,005	0,006	0,007	0,008	0,009	0,01	0,011	0,012
2%	56	50	45	39	34	25	19	15	11	8	4	0	0
4%	73	67	61	49	42	33	25	18	12	6	3	1	0
6%	81	72	41	31	26	18	11	5	1	0	0	0	0
8%	87	72	29	21	11	6	3	0	0	0	0	0	0
10%	91	69	15	13	7	0	0	0	0	0	0	0	0
12%	92	61	16	7	1	0	0	0	0	0	0	0	0

ENTSO-E AISBL • Avenue Cortenbergh 100 • 1000 Brussels • Belgium • Tel +32 2 741 09 50 • Fax +32 2 741 09 51 • info@entsoe.eu • www.entsoe.eu

TABLE 8. QUALIFIED COMBINATIONS (MAXIMUM 72) OF TI AND KP FOR VARYING BACKLASH AND DROOP.

50s	Ti \ Kp	1	2	3	4	5	6	7	8	9	10
	10	0	0	0	0	0	1	2	2	3	4
	20	0	4	8	10	12	10	12	14	15	17
	30	2	7	12	16	18	17	19	21	22	24
	40	2	7	13	17	18	18	22	21	22	24
	50	0	3	4	5	4	5	7	7	8	10
	60	0	0	0	0	0	0	0	0	1	2
	70	0	0	0	0	0	0	0	0	0	1
	80	0	0	0	0	0	0	0	0	0	0
	90	0	0	0	0	0	0	0	0	0	0
	100	0	0	0	0	0	0	0	0	0	0

60s	Ti \ Kp	1	2	3	4	5	6	7	8	9	10
	10	0	0	0	0	0	1	2	2	3	4
	20	0	4	8	10	12	10	12	14	15	17
	30	2	7	12	16	18	17	19	21	22	24
	40	3	9	15	21	23	23	26	26	26	27
	50	3	8	14	17	20	19	22	22	23	24
	60	1	4	5	7	6	9	11	13	13	14
	70	0	0	0	0	0	1	1	3	5	6
	80	0	0	0	0	0	0	1	2	3	4
	90	0	0	0	0	0	0	0	1	2	4
	100	0	0	0	0	0	0	0	1	2	3

70s	Ti \ Kp	1	2	3	4	5	6	7	8	9	10
	10	0	0	0	0	0	1	2	2	3	4
	20	0	4	8	10	12	10	12	14	15	17
	30	2	7	12	16	18	17	19	21	22	24
	40	3	10	18	24	25	25	28	27	27	28
	50	4	10	16	22	24	26	26	27	27	28
	60	3	9	14	20	19	23	22	24	22	23
	70	2	4	6	8	11	12	13	15	16	16
	80	0	0	0	0	1	3	5	6	7	8
	90	0	0	0	0	0	1	3	5	6	6
	100	0	0	0	0	0	1	3	4	5	6

80s	Ti \ Kp	1	2	3	4	5	6	7	8	9	10
	10	0	0	0	0	0	1	2	2	3	4
	20	0	4	8	10	12	10	12	14	15	17
	30	2	7	12	16	18	17	19	21	22	24
	40	3	10	18	24	25	25	28	27	27	28
	50	4	12	20	26	27	29	30	29	29	30
	60	4	10	17	24	26	27	28	29	27	28
	70	4	9	16	20	20	24	23	25	24	24
	80	3	6	10	12	12	16	16	18	17	17
	90	0	0	0	2	4	6	7	8	8	9
	100	0	0	0	1	2	5	6	7	8	8

90s	Ti \ Kp	1	2	3	4	5	6	7	8	9	10
	10	0	0	0	0	0	1	2	2	3	4
	20	0	4	8	10	12	10	12	14	15	17
	30	2	7	12	16	18	17	19	21	22	24
	40	3	10	18	24	25	25	28	27	27	28
	50	4	12	20	26	27	29	30	29	29	31
	60	4	13	20	27	28	30	30	32	30	30
	70	4	13	19	26	25	28	28	30	28	29
	80	4	9	16	19	21	24	23	25	24	24
	90	3	6	10	12	15	16	17	19	17	18
	100	0	0	2	5	6	9	9	11	10	11

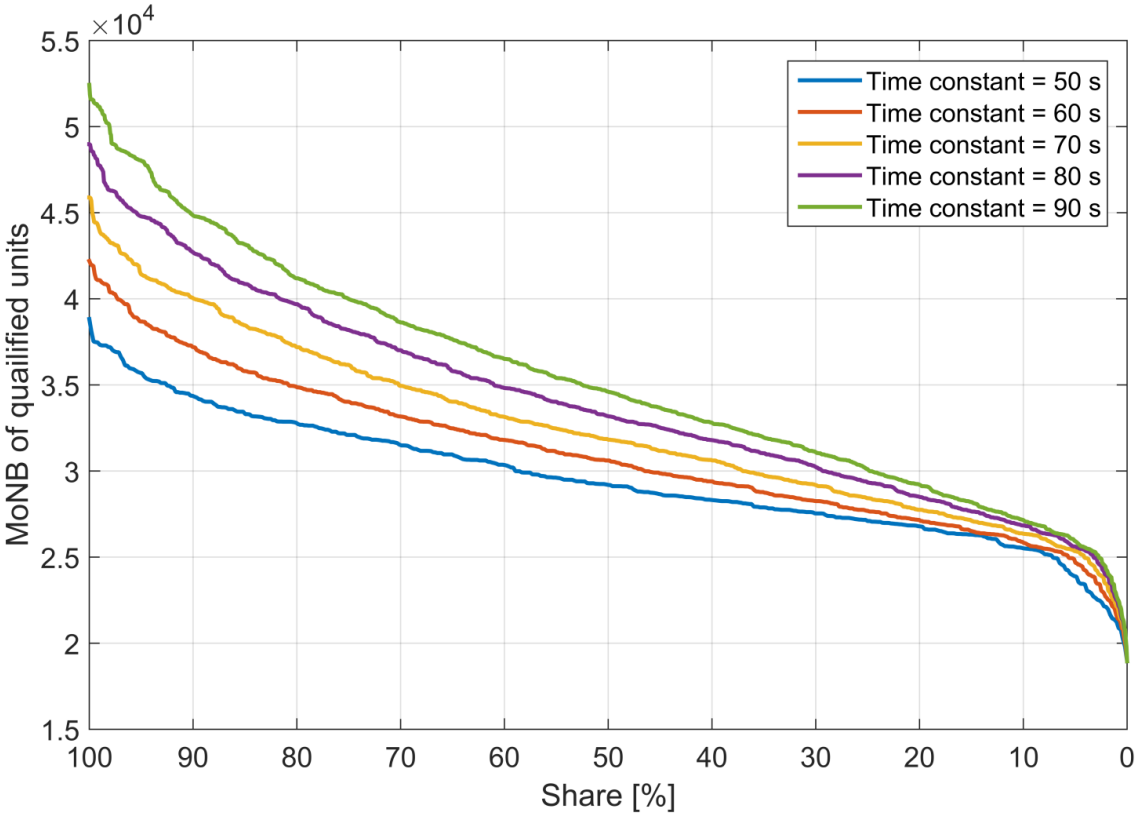

FIGURE 20. DURATION CURVE OF MONB USING DIFFERENT DISTURBANCE FILTER TIME CONSTANT AND A VOLUME OF 600 MW FCR-N.

As described in Appendix there is a clear relation between the resonance peak of the sensitivity function and the minutes outside normal band. Moreover, the performance requirement was designed not to let a disturbance result in too high output even though the minutes outside on average are acceptable. Figure 21 shows two sets of K_p and K_i parameters where the non-qualified unit fails at a particular time period but performs better in terms of minutes outside normal band than a qualified unit.

ENTSO-E AISBL • Avenue Cortenbergh 100 • 1000 Brussels • Belgium • Tel +32 2 741 09 50 • Fax +32 2 741 09 51 • info@entsoe.eu • www.entsoe.eu

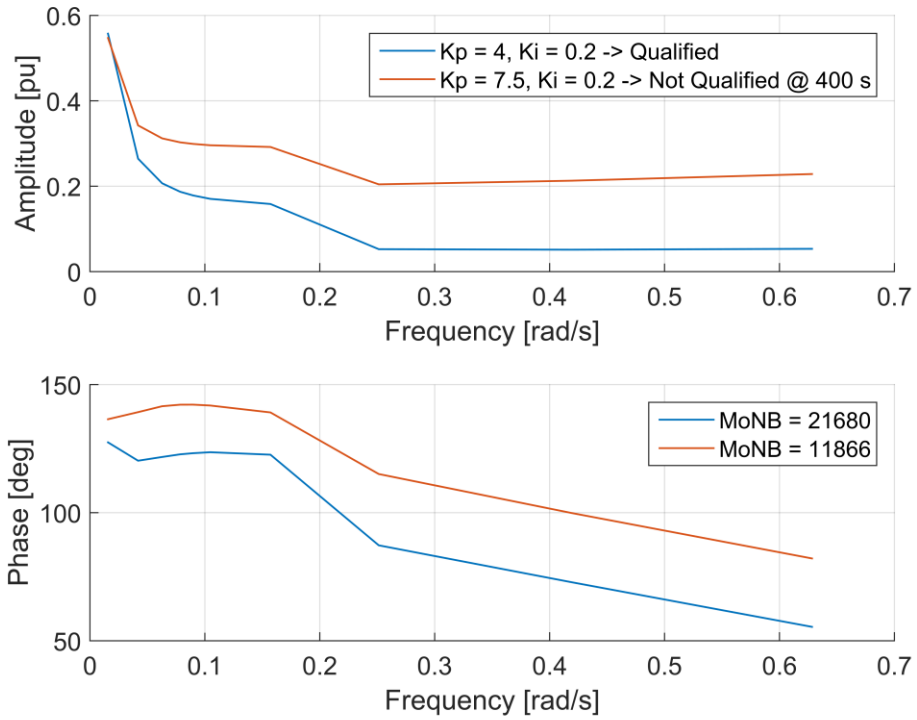

FIGURE 21. EXAMPLE OF QUALIFIED AND NON-QUALIFIED UNIT.

Figure 22 shows qualified and non-qualified sets of parameters for a unit with 2 % droop and varying backlash. Clearly, on average the qualified units perform much better in terms of minutes outside normal band than non-qualified units. As expected, including non-linearities show that there is no clean cut between qualified and non-qualified units and sets of parameters. Also there is a difference coming from the quantification of MoNB, which is rather rough, and the fact that quantifying measures in the time and frequency domain have different objectives. One aim has been to reduce the overlap which is also a reason for choosing the 70 second time constant of the disturbance filter.

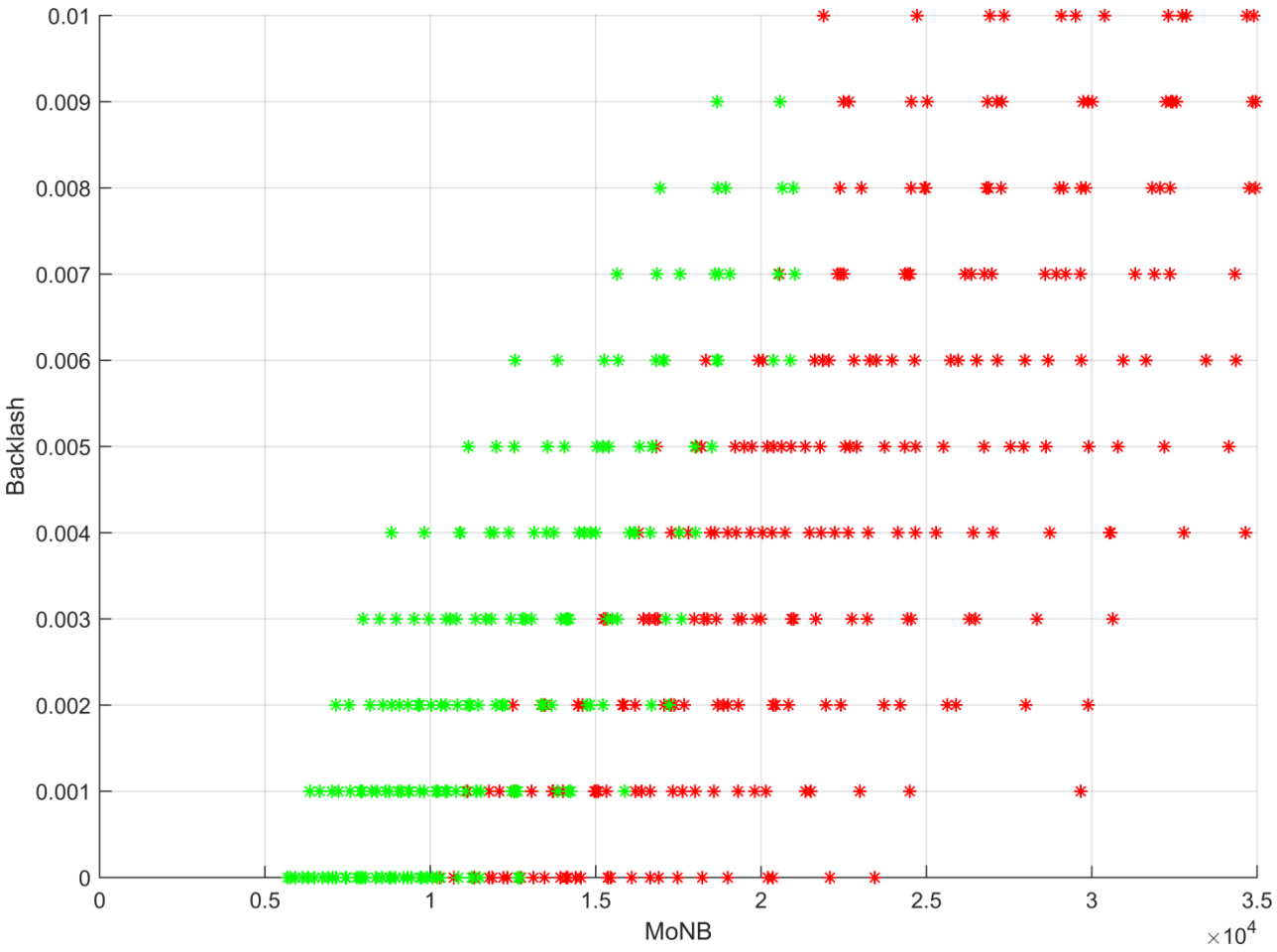

FIGURE 22. GREEN MARK INDICATES A QUALIFIED SET OF K_P AND K_I PARAMETERS, WHEREAS RED IS NOT QUALIFIED FOR A UNIT WITH 2% DROOP.

Main point: To summarise, requirements are stated in terms of

- limits on the sensitivity function and , given by

$\left|S_{\text{avg}}(s)\right| < \left|\frac{70s+1}{6000G_{\text{avg}}(s)}\right|$ and

- Robust stability in the Nyquist plane $G_{\text{o-avg}}(j\omega)$ not entering the stability circle nor encircles the point -1
- the signal strength shall have an amplitude of 100 mHz.

ENTSO-E AISBL • Avenue Cortenbergh 100 • 1000 Brussels • Belgium • Tel +32 2 741 09 50 • Fax +32 2 741 09 51 • info@entsoe.eu • www.entsoe.eu

4.4 DIFFERENT METHODS TO CHECK STABILITY AND PERFORMANCE

There are different ways to evaluate stability and performance, here three different ways are stated. Table 9 gives an overview of how to express the requirements. The grey cells indicate the selected methods for stability and performance, respectively. Note that both stability and performance requirements have to be fulfilled at the same time. The main advantage of sensitivity is the firm limitations for both stability and performance. As will be seen for Nyquist (performance) and FCR-plane the limitation cannot be combined and visualised in a single plot, rather snap shot at discrete frequencies. An advantage with the FCR-plane is that the control response vector is standalone plotted.

TABLE 9. THREE DIFFERENT EXPRESSIONS FOR REQUIREMENTS ON STABILITY AND PERFORMANCE.

	Stability	**Performance**
A. Sensitivity	**S–A.** $\lvert S_{\min}(s)\rvert < M_s$ [vi]	**P–A.** $\lvert S_{avg}(s)\rvert < \frac{\sigma_f}{\lvert D(s)G_{\text{avg}}(s)\rvert}$
B. Nyquist	S–B. $\lvert -F(s)^{\text{vii}}G(s)+1\rvert > \frac{1}{M_s}$	**P–B.** $\lvert -F(s)^{\text{vii}}G_{\text{avg}}(s)+1\rvert > \frac{\lvert D(s)G_{\text{avg}}(s)\rvert}{\lvert\sigma_f\rvert}$
C. FCR-plane	**S–C.** $\left\lvert F(s)^{\text{vii}} - \frac{1}{G_{\min}(s)}\right\rvert > \frac{1}{M_s\lvert G_{\min}(s)\rvert}$ [vi]	**P–C.** $\left\lvert F(s)^{\text{vii}} - \frac{1}{G_{\text{avg}}(s)}\right\rvert > \frac{\lvert D\rvert}{\lvert\sigma_f\rvert}$

The requirements are translated into a requirement of power plant performance and stability in order to be tested and verified locally at each FCR provider "$F(s = j\omega)$". The FCR-N response is defined by internally apply the negative feedback, shown in Figure 23. This implies the loop gain to be re-defined as

$$G_0(s) = -G(s) \cdot (-F(s)) \tag{4.13}$$

which is equivalent of a phase shift of 180°. For sensitivity or Nyquist the positive feedback is handled by simple phase shift the FCR response by 180°. The method mapped to the FCR-plane considered the sign in the derivation.

[vi] This holds if nominal stability is ensured

[vii] Note, the FCR response is here defined with positive feedback and the negative sign included in the internal response.

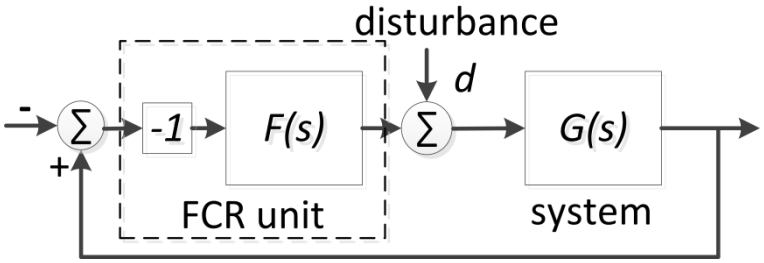

FIGURE 23. FCR-N UNIT IN POSITIVE FEEDBACK.

A. SENSITIVITY

Sensitivity has been described and it is used as the starting point to develop performance in the Nyquist and FCR-plane. This is a common way to describe combined requirements of Euclidian norm for stability and rejection of disturbances.

B. THE NYQUIST PLANE

Stability in the Nyquist plane was explained in Section 2.1. The performance requirement can also be expressed in the Nyquist plane. The requirement in (4.11) is re-written as

$$|F(s)G(s)+1| > \left|\frac{D(s)G_{\mathrm{avg}}(s)}{\sigma_{\mathrm{f}}}\right| = |r_{\mathrm{p}}(s)|. \qquad (4.14)$$

Thus, to fulfil the performance requirement the Nyquist curve shall stay outside the Nyquist performance circles $r_{\mathrm{p}}(s)$ for all frequencies. Thus, circles centred at the point -1 with various radiuses – each point (frequency) of the Nyquist must lie outside the corresponding circle. An example is plotted in Figure 24 with two different performance circles in addition to the firm stability circle.

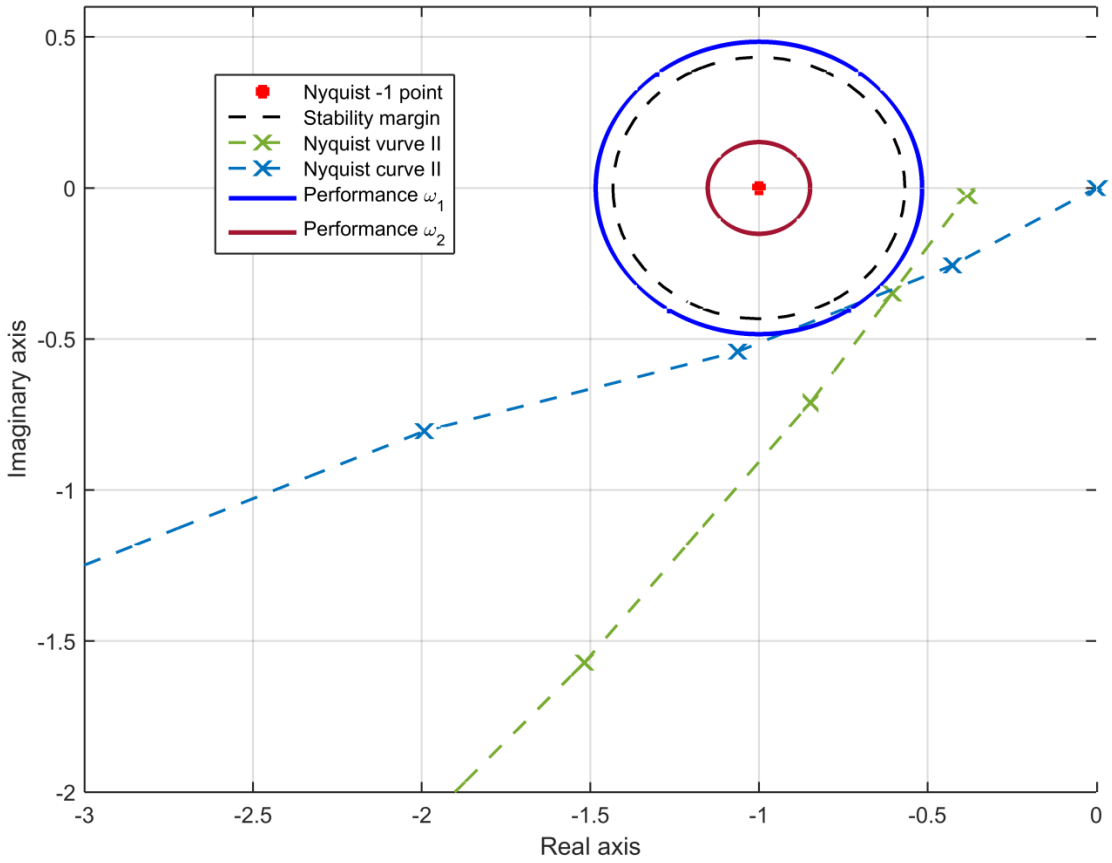

FIGURE 24. NYQUIST DIAGRAM FOR TWO DIFFERENT UNITS. BLACK CIRCLE IS THE STABILITY REQUIREMENT AND BLUE AND DARK RED ARE PERFORMANCE REQUIREMENTS AT DIFFERENT TIME PERIODS.

C. THE FCR-PLANE

The FCR-plane[viii] is a mapping of the requirement expressed in sensitivity to an FCR response (FCR-vector). The absolute value of the sensitivity function $S(j\omega)$ can be expressed as the inverse of the distance between a Nyquist curve and the point -1. The FCR function is given with positive feedback, thus the sensitivity function is rearranged to

$$|S(s)| = \frac{1}{|G_O(s)-(-1)|} = \frac{1}{|-F(s)\cdot G(s)-(-1)|}. \tag{4.15}$$

This knowledge combined with (4.3) can be re-written on the form

$$\left|F(s) - \frac{1}{G_{\min}(s)}\right| > \frac{1}{M_s|G_{\min}(s)|}. \tag{4.16}$$

The performance requirement expressed in (4.11) is re-rewritten to

$$\left|F(s) - \frac{1}{G_{avg}(s)}\right| > \frac{|D(s)|}{|\sigma_f|}. \tag{4.17}$$

This can be interpreted as the joint response of all FCR providers and the controlled system that they together should have a stronger response than the disturbance vs. frequency quality target

[viii] For more information on M-circles please see [7]

that is required, with phase shift considered. The controlled system's load frequency dependency continuously helps to dampen the effects of the active power disturbances whereas the system inertia reduces the additional work required by the FCR providers only at short period times. The same holds for stability margins but here the total system response should be larger than a different value.

The technical implications of (4.16)-(4.17) is that the FCR response, $F(j\omega)$, is a complex valued function of ω. With the FCR response being complex valued this entails that it can be depicted as a vector in the complex plane. Then this implies that the distance between the vectors $F(j\omega)$ and $\frac{1}{G(j\omega)}$, which is also complex valued, must be greater than a certain value, $\frac{|D(j\omega)|}{|\sigma_f|}$ for performance and $\frac{1}{M_s|G_{\min}(j\omega)|}$ *for* stability margins. In graphical terms this implies that the FCR vector must point outside a circle with the radius of $\frac{|D(j\omega)|}{|\sigma_f|}$ or $\frac{1}{M_s|G_{\min}(j\omega)|}$ with their centre at $\frac{1}{G_{avg}(j\omega)}$ and $\frac{1}{G_{\min}(j\omega)}$, as shown in Figure 25 . This implies the radius and the centre of the circle are a function of frequency ($j\omega$). Hence, the circles move around in the FCR-plane and can only be visualised at discrete frequencies, exemplified in Figure 26.

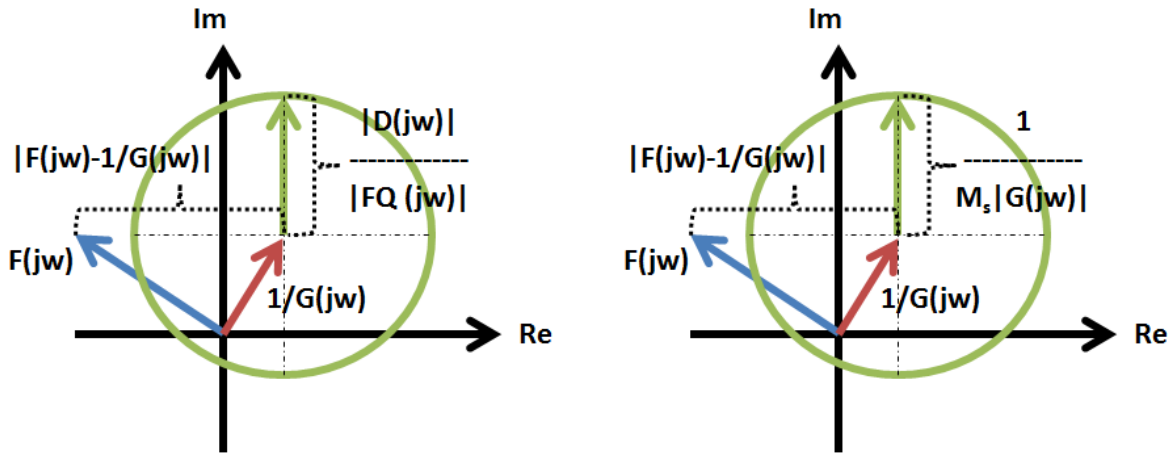

FIGURE 25. GRAPHIC INTERPRETATION OF THE REQUIREMENT STATED IN (4.17) WITH PERFORMANCE REQ. SHOWN TO THE LEFT AND STABILITY MARGINS REQ. SHOWN TO THE RIGHT. THE FCR PROVIDER "$F(j\omega)$" FULFILS THE REQUIREMENT IN (4.16) IF THE $F(j\omega)$-VECTOR POINTS "OUTSIDE" THE GREEN CIRCLES.

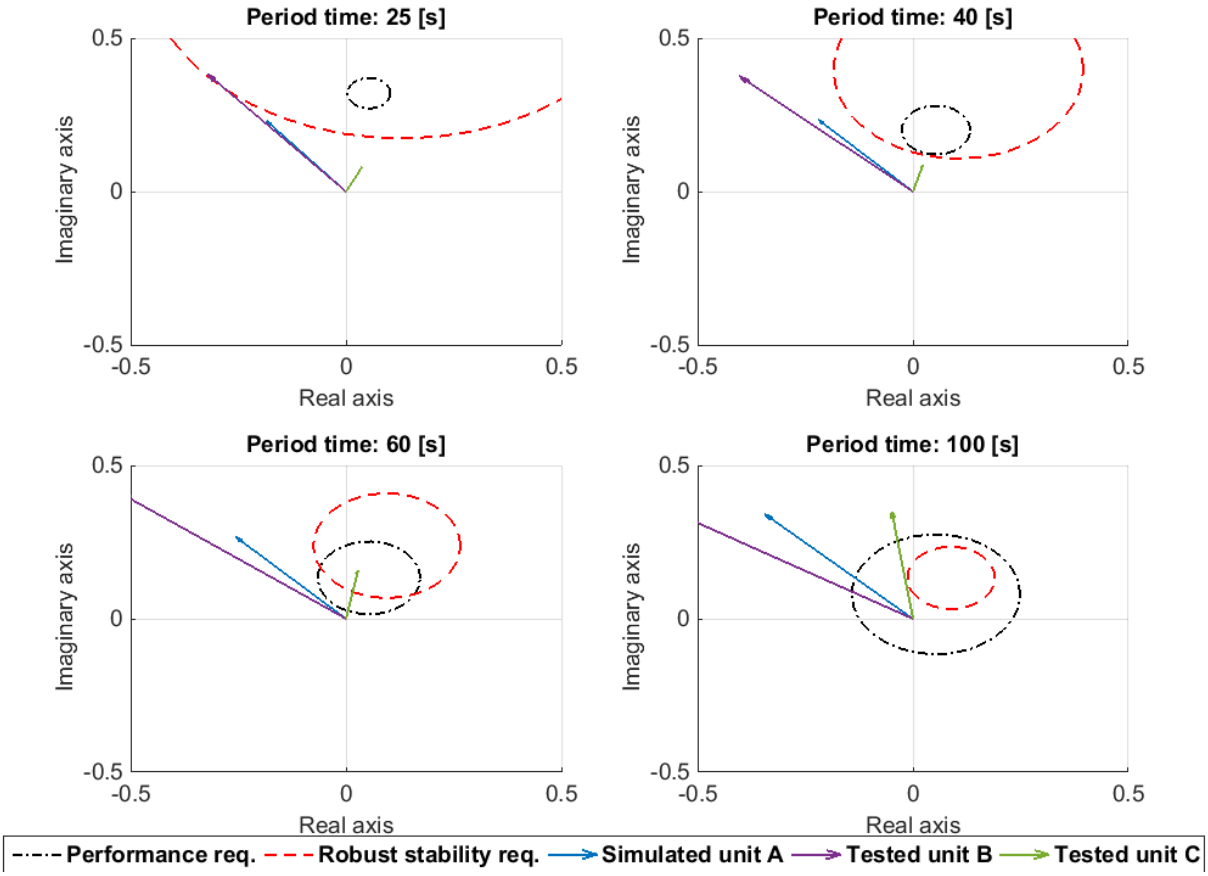

FIGURE 26. VISUALISATION OF THE THREE FCR-VECTORS FOR DIFFERENT TIME PERIODS.

5. TEST PROCEDURE

In a simulation model one can perform the testing in a continuous manner. However, real testing requires testing at discrete and finite number of test periods of the injected sinusoidal. Stability and performance requirements specify limits on the sensitivity functions specified on the total system (for G_{min} and G_{avg}). The aim of the requirements on an FCR-N provider is that an individual unit shall be able to be tested locally on site. The performance and stability requirements described above are not expressed on such form. Per unit scaling simplifies the performance requirement to $\left|S_{\mathrm{avg}}(s)\right|_{\mathrm{pu}} < \left|\frac{70s+1}{G_{\mathrm{avg}}(s)}\right|$.

This can be done since the regulating strength is 6000 MW/Hz and this is then one per unit.

The beauty of using per unit comes at the point of testing different units as no rescaling from per unit on individual power bases is necessary. Recall definition of the loop gain as G(s) times F(s). The static gain of an FCR provider *x* is $F_{\mathrm{x}}(j0)$ and the number n_{x} time the static unit response shall result in the total gain of dP, i.e.

$$F_x(j0)n_x = dP \tag{5.1}$$

Then the loop gain can be written as

$$G(s)F(s) = G(s)\cdot F_x(s)\cdot n_x = G(s)\cdot F_x(s)\cdot n_x \frac{F_x(j0)\cdot n_x}{F_x(j0)\cdot n_x} = G(s)\cdot F_x(s)\cdot n_x \frac{dP}{F_x(j0)\cdot n_x} =$$

$$= G(s)\cdot dP \cdot \frac{F_x(s)}{F_x(j0)} = G_{pu}(s)\cdot \frac{F_x(s)}{F_x(j0)} \tag{5.2}$$

Note that the system expressed in physical units is scaled to per unit by *dP*. The last term is the per unit scaling of an individual unit and it is clear that the requirements can be mapped to the per unit response of a unit with any capacity contribution.

5.1 FCR-N CAPACITY AND PREQUALIFICATION NORMALISATION

FCR providing entities controlled via mechanical equipment like hydro power units, typically have backlash in their mechanical system. This backlash will make the normalisation factor dependent on previous position changes of the control system. Also, backlash visible on the sine test measurements would not be properly taken into account when normalizing the response.

First the capacity of a unit has to be determined by a test procedure. At first, the average of the active power step response shown in Figure 27 is to be found. This is found through a series of step changes in the frequency reference signal. The total backlash in per unit is calculated as

$$2b = \frac{||\Delta P_1| - |\Delta P_2|| + ||\Delta P_3| - |\Delta P_4||}{2} \tag{5.3}$$

and the capacity is reduced by *b* from the backlash. The capacity that can be qualified and sold is the average calculated as

$$C_x = \frac{|\Delta P_1| + |\Delta P_2| + |\Delta P_3| + |\Delta P_4|}{4} \tag{5.4}$$

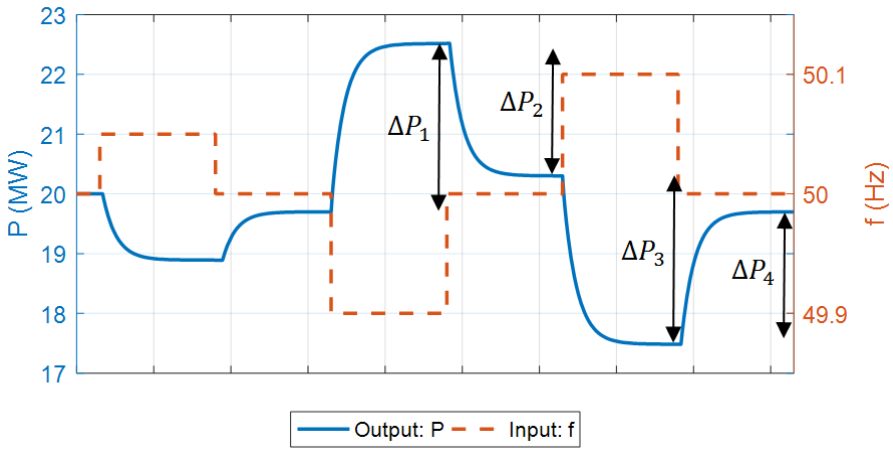

FIGURE 27. FCR-N STEP RESPONSE SEQUENCE

The total backlash is not allowed to be above 30 % of the total capacity.

In order to make the unit independent of the FCR capacity normalisation is performed. The normalisation is defined so that the static gain shall be equal to one per unit, i.e.

$$\left|F_{x-pu}(j0)\right| = 1 \text{ pu} \tag{5.5}$$

The normalisation consists of two steps, first backlash is to be found and secondly the fundamental component scaling has to be included.

Hence, the normalized gain of the transfer function for any angular frequency ω can be calculated as

$$|F_{x-\text{pu}}(j\omega)| = \frac{|FCR_x(j\omega)|}{e_x} \tag{5.6}$$

where *e* is the normalization factor.

The normalisation factor, *e*, is given by

$$e = e_{x-1}e_{x-2} \tag{5.7}$$

where $e_{x-1} = C_x$ and e_{x-2} is α(ΔP,b) as given in Table 3.

In order to estimate the frequency response of a unit sine-in-sine-out tests are performed. To cover the most important frequencies ten time periods were chosen to be tested, these are

Time periods, T = [300, 150, 100, 80, 70, 60, 50, 40, 25, 15, 10] s

and the corresponding angular frequencies are given by $\omega = \frac{2\pi}{T}$. (5.8)

The frequency deviation signal is manipulated by the sinusoidal frequency signal and the output power is measured, see Figure 28. The phase ϕ (in degrees) of the transfer function for a certain angular frequency / time period can be calculated as

$$\phi = \text{Arg}(-F(j\omega)) = \Delta t \frac{360°}{T} \tag{5.9}$$

where *T* is the time period (s) and Δt is the time difference (s) of the input (frequency) signal and output (power) signal, as shown in Figure 28.

To allow some uncertainty during real tests the true requirement is set to 95 % at each time period. This would allow for 5 % error for stability or performance. The radius of the stability circle in the Nyquist plane in reduced by 5 % and so is each performance circle.

ENTSO-E AISBL • Avenue Cortenbergh 100 • 1000 Brussels • Belgium • Tel +32 2 741 09 50 • Fax +32 2 741 09 51 • info@entsoe.eu • www.entsoe.eu

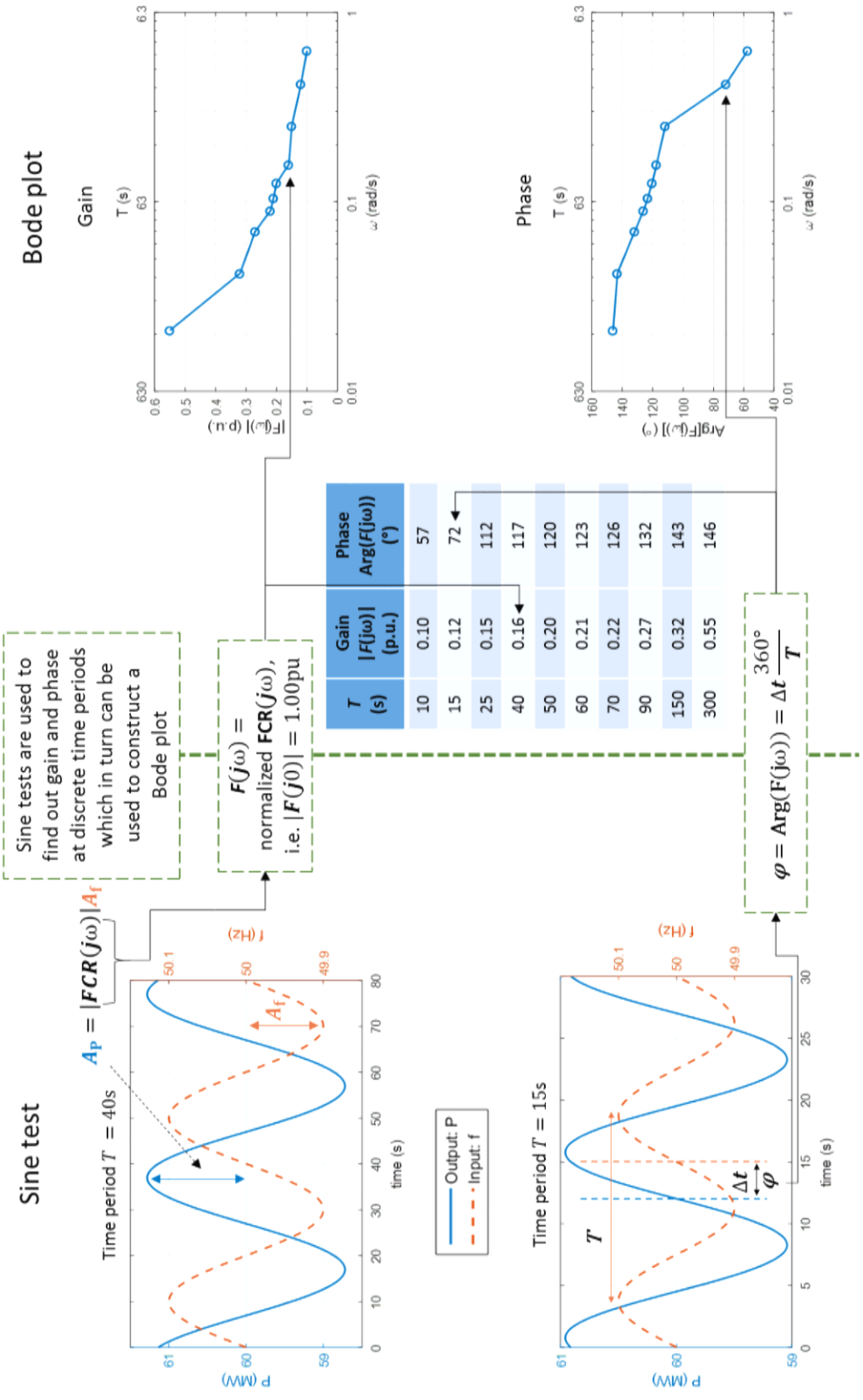

FIGURE 28. SINE TESTS, TRANSFER FUNCTION VALUES AND BODE PLOTS.

6. CONCLUSIONS

This work describes the new requirements that have been developed for the frequency containment reserve for normal operation, FCR-N. The main aim was to develop new requirements that improve the frequency quality in the Nordic synchronous area. Moreover, the requirements shall be expressed such that they can be implemented in a unified manner. New requirements have been developed which are testable locally on site by performing step and sine-in-sine-out tests. The requirements are expressed in stability and performance requirement which are combined. These can be expressed in terms of limit on the sensitivity function, Nyquist plane or FCR-plane. Stability is expressed with a margin in order to maintain stability with uncertainties included. Performance is expressed in terms of amplification from a disturbance, at any frequency, to the impact on the output frequency quality.

7. REFERENCES

[1] H. Nyquist, ”Regeneration theory,” *The Bell System Technical Journal*, pp. 126-147, 1932.

[2] ”Description of Nordic frequency model,” Control design working group, 2017.

[3] T. Ellefsrød, ”Nordic Grid - FNR Frequency Containment, Generating equipment performance - review report,” Norconsult, 2016.

[4] S. Skogestad och I. Postlethwaite, Multivariable Feedback Control, 2nd red., Wiley, 2005.

[5] ”Imbalance study SE3-4,” Control design working group, Sundbyberg, 2016.

[6] ” DESCRIPTION OF NORDIC FREQUENCY MODEL", Control design working group, 2017.

[7] T. Hägglund och K. J. Åström, Advanced PID Control, ISA-The Instrumentation, Systems, and Automation Society, 2006.

8. APPENDIX A – LIST OF APPENDICES IN THE FCR-N DESIGN OF REQUIREMENTS

Supporting documents produced during the FCR-N design are listed below.

8.1 PRE-QUALIFICATION DOCUMENT

8.1.1 “TECHNICAL REQUIREMENTS FOR FREQUENCY CONTAINMENT RESERVE PROVISION IN THE NORDIC SYNCHRONOUS AREA V1.1”

ENTSO-E AISBL • Avenue Cortenbergh 100 • 1000 Brussels • Belgium • Tel +32 2 741 09 50 • Fax +32 2 741 09 51 • info@entsoe.eu • www.entsoe.eu

The technical Requirements for Frequency Containment Reserve Provision in the Nordic Synchronous Area specify formal technical requirements for Frequency Containment Reserve (FCR) providers as well as requirements for compliance verification and information exchange. The requirements are based on SOGL 1, with proper adjustments to be suitable for the Nordic conditions.

8.1.2 „Supporting Document on Technical Requirements for Frequency Containment Reserve Provision in the Nordic Synchronous Area“

The supporting Document on Technical Requirements for Frequency Containment Reserve Provision in the Nordic Synchronous Area contains material to support the interpretation of these technical requirements.

8.2 “Description of Nordic Frequency Model“, Control design working group, Fredericia, 2017

In this document the time domain model for simulating the frequency behavior of the Nordic Synchronous system is described. The model is based on the initial model developed for the Nordic project called “RAR” which was conducted in 20.

8.3 “Parameter Sensitivity Study, Final design with 70s profile“, Control design working group, Fredericia, 2017

In this document the proposed optimum governor parameters are tested for robustness against variations in the most dominant system- and unit parameters in the simulation model described in section 8.2.

8.4 “ Power Plant Qualification study, Final design with 70s profile“, Control design working group, Fredericia, 2017

This document reports on the results from simulations of a pre-qualification study of a hydro power plant according to the performance specification of the FCR-N as described in section 8.1. The simulations were performed with the Nordic Frequency model described in section 8.2.

8.5 “System Performance Study, Final design with 70s profile“, Control design working group, Fredericia, 2017

In this document the system frequency performance obtained with the new FCR-N requirements as defined by section 8.1 is compared with the system frequency performance of the existing Nordic FCR-N reserves anno 2017.

ENTSO-E AISBL • Avenue Cortenbergh 100 • 1000 Brussels • Belgium • Tel +32 2 741 09 50 • Fax +32 2 741 09 51 • info@entsoe.eu • www.entsoe.eu

8.6 "IMBALANCE STUDY SE3-4", CONTROL DESIGN WORKING GROUP, SUNDBYBERG, 2016

This document describes the estimation of the stochastic net-power variations in the Nordic synchronous area. Measurements from energy meters were achieved in an area and then scaled to represent to total Nordic synchronous area.

8.7 "OPTIMISATION" (APPENDIX B IN THIS REPORT)

This appendix describes an optimizing routine developed on a simplified linear model. The routine uses different hard and soft tuning targets to develop an optimized parameter settings on the turbine governor.

9. APPENDIX B – LINEAR OPTIMISATION

An optimization routine was created for the linear model where the performance and stability requirements were imposed as hard tuning target. In addition to these hard targets two different soft targets were created in order to be able to test different realizations of a system that abides by the hard targets. The hard and soft targets are implemented in the optimization routine as follows

$$\begin{cases} \textbf{Optimization} = \\ \begin{cases} \left\| S(j\omega)_{avg.} \frac{G(j\omega)D(j\omega)}{fq(j\omega)} \right\|_\infty < 1, \ \textbf{Hard: Performance} \\ \|S(j\omega)_{min} * M_s\|_\infty < 1, \ \textbf{Hard: Stability} \end{cases} \\ min \begin{cases} \left\| \frac{F(j\omega) * (K * j\omega)}{G(j\omega)_{avg} S(j\omega)_{avg}} \right\|_\infty < 1 & , \ \textbf{Soft: Limit FCR } \omega_B \\ & , \ \textbf{Soft: Limit resonance peak} \end{cases} \end{cases} \quad (29)$$

THE OPTIMIZATION ROUTINE STATES THAT FOR THE HARD TUNING TARGET THE REQUIREMENT SHALL BE MET WHEREAS FOR THE SOFT TARGET THEY SHALL BE MINIMIZED.

The soft targets are developed to i) minimize the open-loop bandwidth of an FCR-N provider from grid frequency input to active power output and ii) minimize the resonance peak of the closed-loop system from power disturbances to grid frequency deviations. Varying the factor *K* in the soft target for bandwidth limitation allows the routine to develop different system configurations / parameterizations that can be evaluated against each other.

Two different simulations have been attempted

i. Four different hard performance requirements have been tested combined with varying the *K-factor*. The intention with varying the K-factor is that it will realize the system from one extreme point (slow FCR response) to another extreme point (minimized resonance peak).

ii. Ten different hard performance requirements have been tested combined with a fixed *K-factor* (minimize FCR-N bandwidth). The hard performance requirement is here tested with 600 MW and a time constant that ranges from 10 s to 100 s, in steps of 10 s.

In Figure 30 below an example of an optimization is shown for different transfer functions.

ENTSO-E AISBL • Avenue Cortenbergh 100 • 1000 Brussels • Belgium • Tel +32 2 741 09 50 • Fax +32 2 741 09 51 • info@entsoe.eu • www.entsoe.eu

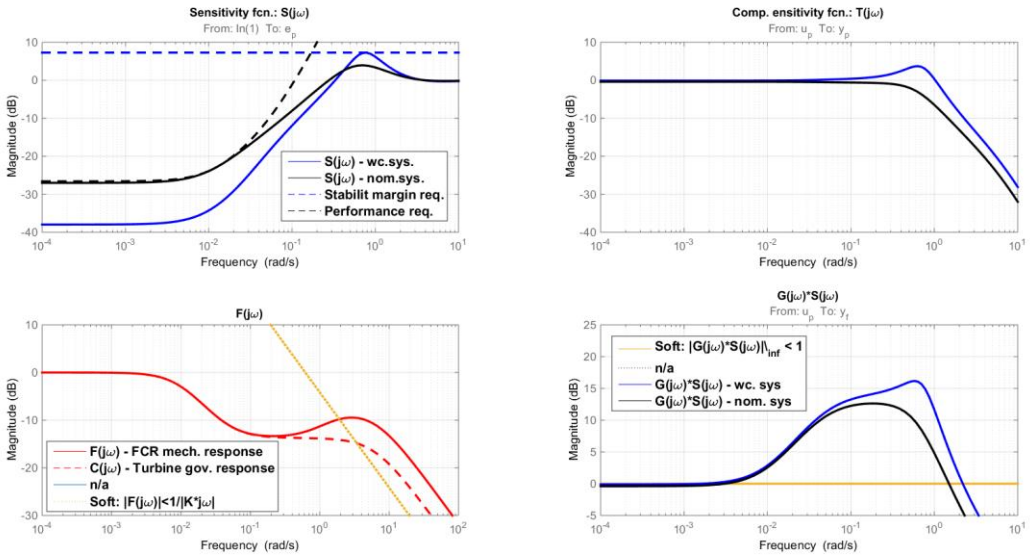

FIGURE 30.SUMMARY PLOT OF DIFFERENT TRANSFER FUNCTIONS DESCRIBING THE OPTIMIZED SYSTEM. FOR THIS PARTICULAR SYSTEM THE PERFORMANCE REQUIREMENT IS MODELLED WITH 900 MW STEADY STATE CAPACITY AND 90S TIME CONSTANT OF THE DISTURBANCE PROFILE. THE K-FACTOR FOR LIMITING FCR-N BANDWIDTH IS SET TO $\frac{1.2^{10}}{10}$ RAD/S.

Optimization for four different scenarios and varying the K-factor

The different systems that are tested are with 600 vs. 900 MW steady state capacity of disturbance with 60 vs. 90 s time constants giving four different scenarios. These are then tested with 20 different K-factors. In to Figure 31 the optimizations are summarized for kpis' in the frequency domain.

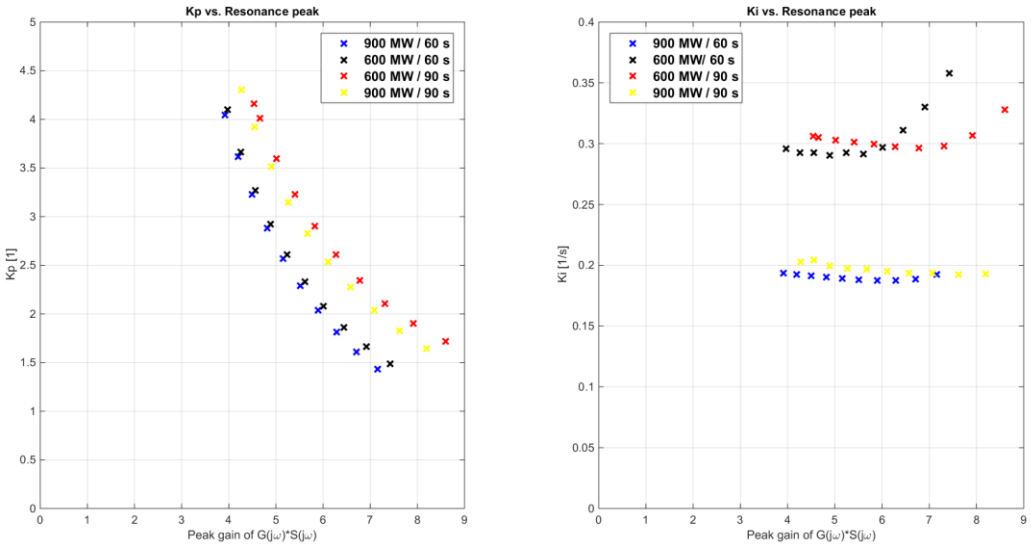

FIGURE 31. PI PARAMETERS FOR AN FCR-N UNIT WITH 6% DROOP PLOTTED AGAINST THE PEAK GAIN OF THE NORMALIZED TRANSFER FUNCTION OF $G * S$.

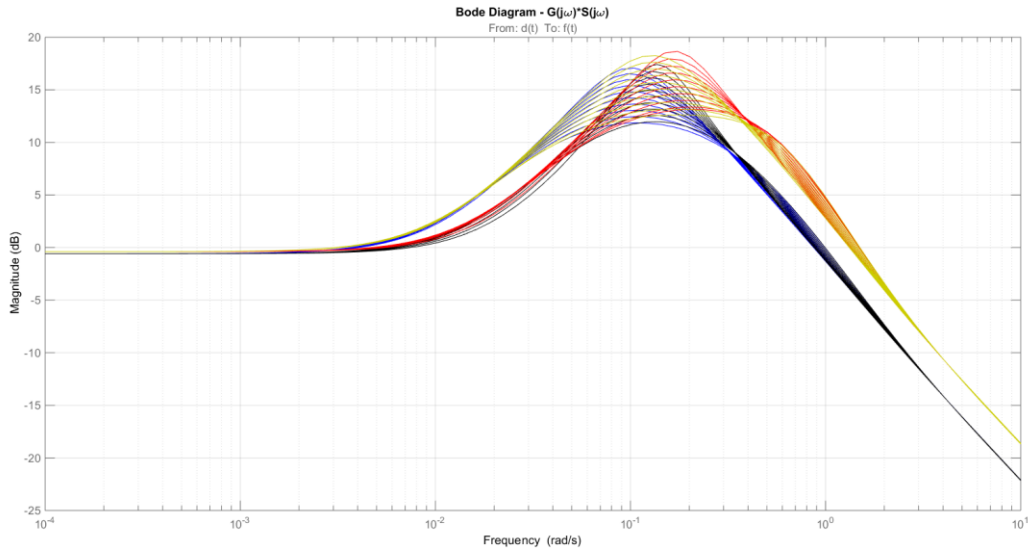

FIGURE 32. BODE MAGNITUDE FOR THE NORMALIZED TRANSFER FUNCTION G*S OF THE NOMINAL SYSTEM. [COLOR = STEADY STATE DISTURBANCE CAPACITY / DISTURBANCE TIME CONSTANT]: BLUE = 900 MW / 60 S, YELLOW = 900 MW, RED = 600 MW / 90 S, BLACK = 600 MW, 60 S.

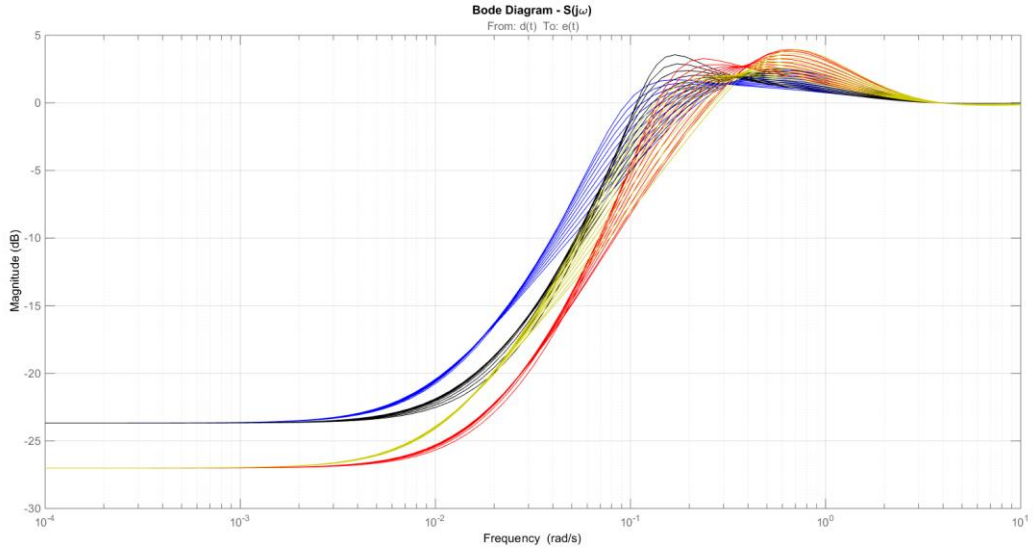

FIGURE 33. BODE MAGNITUDE FOR THE SENSITIVITY TRANSFER FUNCTION, S, OF THE NOMINAL SYSTEM. [COLOR = STEADY STATE DISTURBANCE CAPACITY / DISTURBANCE TIME CONSTANT]: BLUE = 900 MW / 60 S, YELLOW = 900 MW, RED = 600 MW / 90 S, BLACK = 600 MW, 60 S.

Figure 32 shows that the peak gain is higher for a system with a higher static capacity of the disturbance transfer function, *D*. This means that efficiency per MW of FCR-N resource is lower for larger amounts of FCR-N. An example explaining the resonance peak follows below.

D: 900 MW, 90s time constant: $\left\|G(j\omega)_{avg}S(j\omega)_{avg.}\right\|_{\infty} = 8.60\ [p.u.] = 9.60 * 10^{-4}\ [Hz/MW]$

D: 600 MW, 90s time constant: $\left\|G(j\omega)_{avg}S(j\omega)_{avg}\right\|_{\infty} = 7.62\ [p.u.] = 12.4 * 10^{-4}\ [Hz/MW]$

Ratio of peak gains between MW steady state gains and resonance peaks

$$MW_{ratio}: \frac{900}{600} = 1.5\ [p.u.]$$

$$Peak\ gain_{ratio}: \frac{9.60 * 10^{-4}}{12.4 * 10^{-4}} = 0.77\ [p.u.]$$

The ratio between the MW-ratio and the peak gain-ratio shows which system that has the highest MW-efficiency for reducing the total system resonance peak.

$$\eta_{MW} = \frac{MW_{ratio}}{Peak\ gain_{ratio}} = \frac{1.5}{0.77} = 1.95\ [p.u.]$$

The example shows that the 600 MW-system has approximately double the efficiency of suppressing the resonance peak compared to the 900 MW-system per MW of FCR-N capacity. However, the 900 MW-system still suppresses the resonance peak to only 75% of the 600 MW-resonance peak in [Hz/MW].

Optimization for 10 different scenarios and fixed K-factor

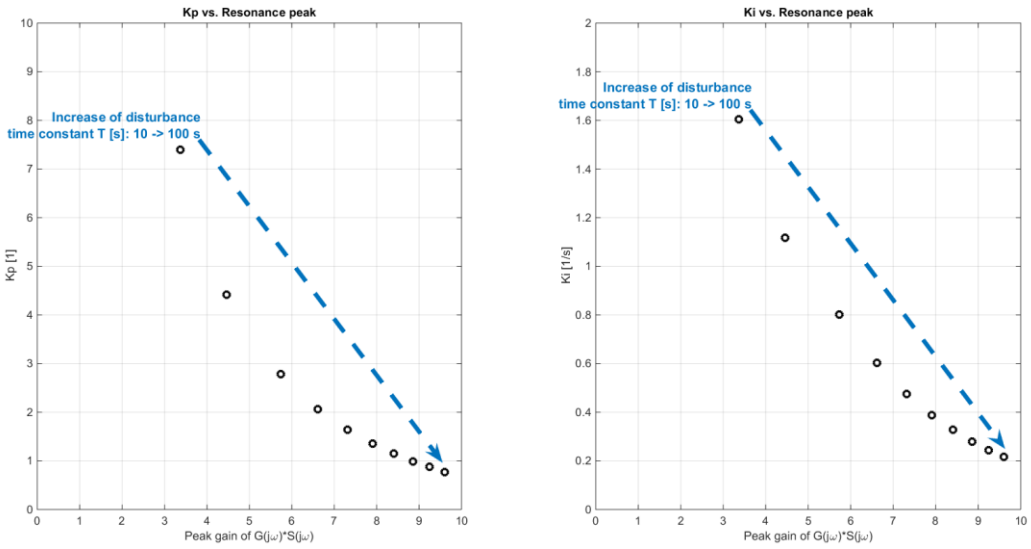

FIGURE 34. PI PARAMETERS FOR AN FCR-N UNIT WITH 6% DROOP PLOTTED AGAINST THE PEAK GAIN OF THE NORMALIZED TRANSFER FUNCTION OF $* S$.

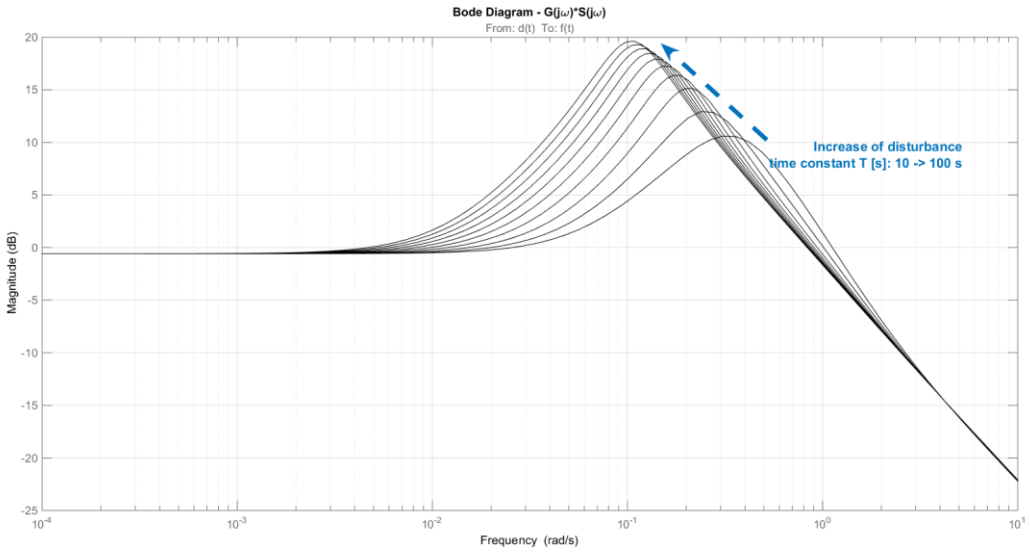

FIGURE 35. BODE MAGNITUDE FOR THE NORMALIZED TRANSFER FUNCTION OF G*S OF THE NOMINAL SYSTEM.

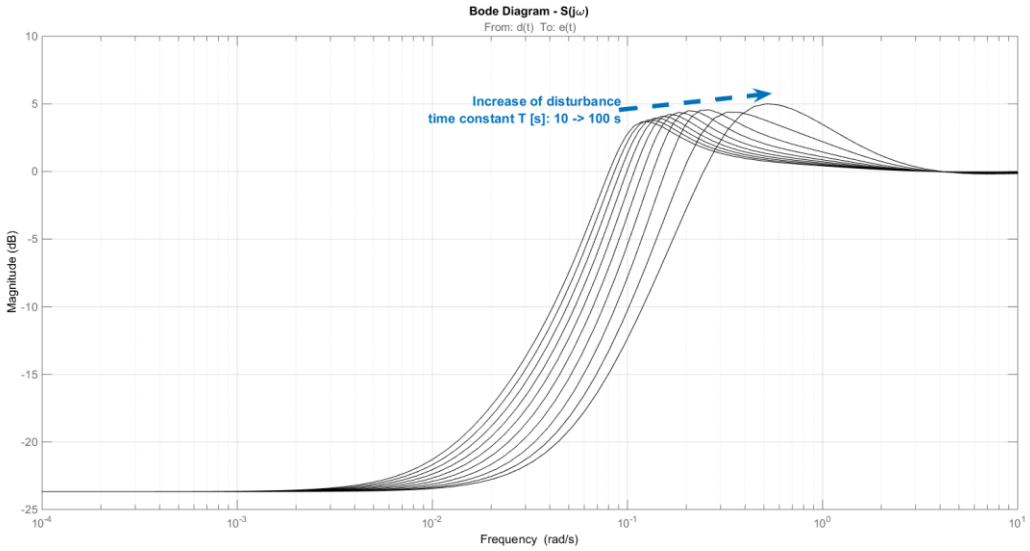

FIGURE 36. BODE MAGNITUDE FOR THE SENSITIVITY TRANSFER FUNCTION, S, OF THE NOMINAL SYSTEM.

Figure 30 to Figure 38 indicate that if the time constant for the disturbance function, D, is decreased then the peak gain of the normalized transfer function of $\boldsymbol{G} * \boldsymbol{S}$ is also decreased and the variance of the physical transfer function of $\hat{\boldsymbol{G}} * \boldsymbol{S}$ is also reduced**.**

Comparisons – Frequency domain vs. time domain

The frequency domain doesn't tell the complete story. Therefore, the system has also been simulated with disturbance time series that were developed in the **RAR-project**. From these simulations, the response in relation to the kpis' is evaluated.

Optimization for four different scenarios and varying the K-factor

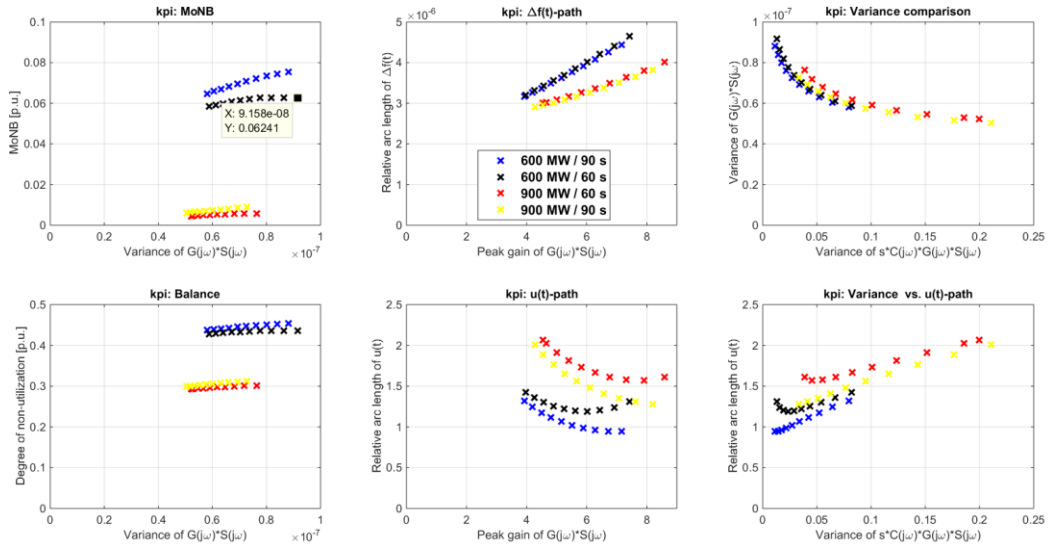

FIGURE 37. SUMMARY OF THE DEVELOPED KPIS' PLOTTED AGAINST EITHER THE PEAK GAIN OF THE NORMALIZED TRANSFER FUNCTION OF $* \boldsymbol{S}$, THE CALCULATED VARIANCE OF THE PHYSICAL SYSTEM OF $\widehat{\boldsymbol{G}} * \boldsymbol{S}$ OR THE VARIANCE OF THE NORMALIZED TRANSFER FUNCTION $\boldsymbol{s} * \boldsymbol{C} * \boldsymbol{G} * \boldsymbol{S}$.

Figure 37 shows some different and interesting things.

KPI: MoNB

i. There is a relationship between the *MoNB* and the variance of the physical transfer function of $\widehat{\boldsymbol{G}} * \boldsymbol{S}$ where a reduction of the variance reduces the kpi.

ii. It is also visible that the total FCR-N steady state capacity here has a positive influence in that it supresses the kpi further.

iii. Further suppression of the kpi is attained if the disturbance time constant is reduced from 90 s to 60 s. The efficiency of the time constant is lower though than an increase in the static capacity (ii).

KPI: Balance

i. There is a relationship between the *MoNB* and the variance of the physical transfer function of $\widehat{\boldsymbol{G}} * \boldsymbol{S}$ where a reduction of the variance reduces the kpi.

ii. It is also visible that the total FCR-N steady state gain here has a positive influence in that it supresses the kpi further.

iii. Further suppression of the kpi is attained if the disturbance time constant is reduced from 90 s to 60 s. The efficiency of the time constant is lower though than an increase in the static capacity (ii).

KPI: Δf(t)-path

i. There is a clear relation between the *relative arc length* of the grid frequency deviation vs the peak gain of the normalized transfer function for $\boldsymbol{G} * \boldsymbol{S}$.

ii. It is also visible that the total FCR-N steady state capacity here has a positive influence in that it supresses the kpi further.

KPI: Δu(t)-path

i. If the total FCR-N steady state capacity is increased then the kpi is increased.

ii. The smaller the resonance peak is for the normalized transfer function $\boldsymbol{G} * \boldsymbol{S}$, the larger the kpi becomes

iii. There seems to be a minimum value for the peak gain where the kpi is at its smallest value

iv. At larger peak gain values the kpi takes on larger values again.

KPI: Variance comparison

i. There seems to be some type of exponential relationship between the variance of the normalized transfer function G*S and s*C*G*S.

KPI: Variance vs. Δu(t)-path

i. There is a general linear relationship between the normalized transfer of s*C*G*S and the relative arc length of the FCR-N controller output.

ii. The linear relationship seems to only hold down to a certain point and then the relative arc length increases.

These kpis' suggests that

i. The more effort that is put in to suppressing the resonance peak the more work an FCR-N provider has to do.

ii. If the FCR-N provider reduces its bandwidth too much giving a large resonance peak then the work performed starts to increase.

iii. The steady state gain of the FCR-N is more important for the *MoNB* and *balance* kpis' than the bandwidth of the FCR-N provider.

Optimization for four different scenarios and varying the K-factor

ENTSO-E AISBL • Avenue Cortenbergh 100 • 1000 Brussels • Belgium • Tel +32 2 741 09 50 • Fax +32 2 741 09 51 • info@entsoe.eu • www.entsoe.eu

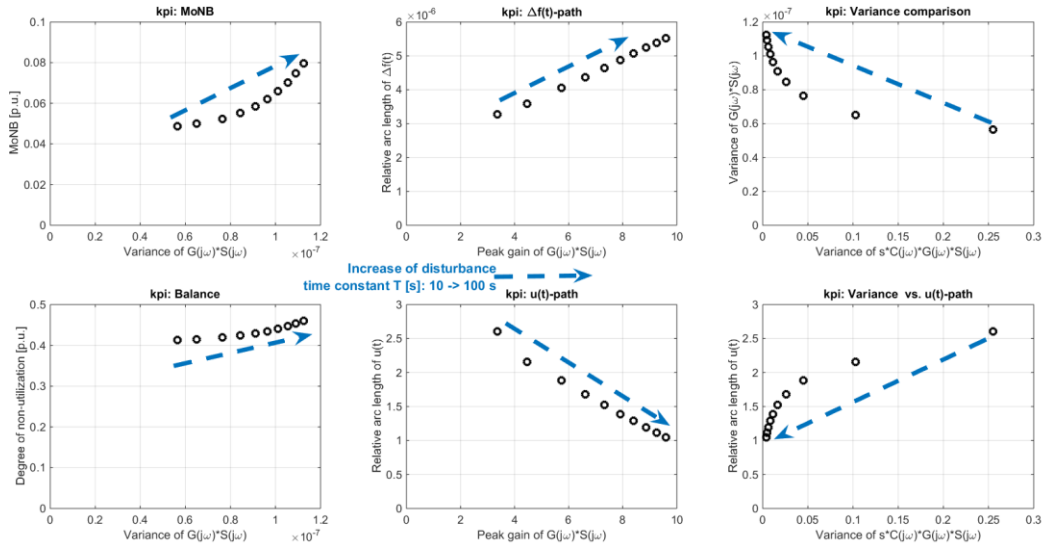

FIGURE 38. SUMMARY OF THE DEVELOPED KPIS' PLOTTED AGAINST EITHER THE PEAK GAIN OF THE NORMALIZED TRANSFER FUNCTION OF $\boldsymbol{G * S}$, THE CALCULATED VARIANCE OF PHYSICAL SYSTEM OF $\boldsymbol{\hat{G} * S}$ OR THE VARIANCE OF THE NORMALIZED TRANSFER FUNCTION OF $\boldsymbol{s * C * G * S}$.

Figure 38 shows some different and interesting things.

KPI: MoNB

i. There is a relationship between the *MoNB* and the variance of the physical transfer function of $\boldsymbol{\hat{G} * S}$ where a reduction of the variance reduces the kpi. It is not linear, however, but seems to be exponential.

KPI: Balance

i. There is a relationship between the *Balance* and the variance of the physical transfer function of $\boldsymbol{\hat{G} * S}$ where a reduction of the variance reduces the kpi. It is not linear however but exponential.

KPI: Δf(t)-path

i. There is a clear relation between the *relative arc length* of the grid frequency deviation vs the peak gain of the normalized transfer function for $\boldsymbol{G * S}$.

KPI: Δu(t)-path

i. There is a clear relation between the *relative arc length* of the FCR-N controller output vs the peak gain of the normalized transfer function for $\boldsymbol{G * S}$.

ii. The more effort that is put in to suppressing the resonance peak the more work and FCR-N provider has to do.

KPI: Variance comparison

i. There seems to be some type of exponential relationship between the variance of the normalized transfer function of G*S and s*C*G*S.

KPI: Variance vs. Δu(t)-path

i. There is a general linear relationship between the normalized transfer of s*C*G*S and the relative arc length of the FCR-N controller output.

ii. The linear relationship seems to only hold down to a certain point and then the relative arc length

These kpis' suggests that

i. The more effort that is put in to suppressing the resonance peak the more work an FCR-N provider has to do.

ii. If the FCR-N provider reduces its bandwidth too much giving a large resonance peak then the work performed again starts to increase.

iii. The steady state gain of the FCR-N is more important for the *MoNB* and *balance* kpis' than the bandwidth of the FCR-N provider.

Discussion on the optimisation

The analysis design approach shows that the design method can improve the frequency quality by either decreasing the time constant of the disturbance function, D, or increasing the steady state gain of the disturbance function, D.

The analysis also shows that there is a trade-off to be made between the arc lengths of the grid frequency and the controller output of an FCR-N unit.

The analysis of the real-life grid frequency deviations indicated that the majority of the energy content lies in a frequency range that is slower than the FCR-N bandwidth. This suggested that the most efficient way to reduce the grid frequency deviations is to increase the system strength by increasing the total FCR-N steady state gain. This was in part confirmed kpi *MoNB* and *Balance*. This also indicates that it is more efficient to include a-FRR to reduce the grid frequency deviations since the a-FRR has an integrating controller which increases the total system strength at frequency lower than the FCR-N bandwidth.

ENTSO-E AISBL • Avenue Cortenbergh 100 • 1000 Brussels • Belgium • Tel +32 2 741 09 50 • Fax +32 2 741 09 51 • info@entsoe.eu • www.entsoe.eu